Inorganica Chimica Acta 421 (2014) 110–122

Contents lists available at ScienceDirect

Inorganica Chimica Acta

journal homepage: www.elsevier.com/locate/ica

New water soluble bis-imidazolium salts with a saldach scaffold: Synthesis, characterization and *in vitro* cytotoxicity/bactericidal studies

Reda F.M. Elshaarawy [a,c,*], Zeinab H. Kheiralla [b], Abeer A. Rushdy [b], Christoph Janiak [c,*]

[a] Faculty of Science, Suez University, Suez, Egypt
[b] Botany Department, University College for Women, Ain Shams University, Cairo, Egypt
[c] Institut für Anorganische Chemie und Strukturchemie, Heinrich-Heine Universität Düsseldorf, 40204 Düsseldorf, Germany

ARTICLE INFO

Article history:
Received 5 April 2014
Received in revised form 21 May 2014
Accepted 26 May 2014
Available online 2 June 2014

Keywords:
Bis-imidazolium salts
Metallosaldach
Cytotoxicity
Antibacterial

ABSTRACT

A series of water-soluble bis-imidazolium salts of the type $H_2(^iPr)_2$saldach(1,2-Me_2Im^+-$X^-)_2$ (**4**) and their mononuclear complexes [M(III)Cl{($^iPr)_2$saldach(1,2-Me_2Im^+-$X^-)_2$}] (M = Mn, **5**; Fe, **6**), (X = Cl, a; PF_6, b; BF_4, c), where saldach = *N*,*N*′-bis(salicylidene)-(±)-*trans*-1,2-diaminocyclohexane, have been synthesized and characterized using elemental analysis, electronic, spectral, magnetic as well as conductometric methods and MALDI-TOF-, ESI-MS. All complexes possess a distorted square pyramidal coordination geometry with MN_2O_2Cl chromophore, as revealed by the elemental, spectral and literature data. These salts have been evaluated for *in vitro* cytotoxicity against HepG-2 and MCF-7 cell lines. Among them, **4**c (IC_{50} = 22.17 μM) exhibited potency against MCF-7. The bactericidal efficacy of **4**a–c was screened against a panel of common pathogenic bacteria. Compound **4**a was found to be the most potent antibacterial agent and could inhibit all the bacterial strains more effectively than standard antibiotics.

© 2014 Elsevier B.V. All rights reserved.

1. Introduction

One of the most chemotherapeutic problems we are facing today in the context of fighting bacterial infectious diseases is the relentless increase and spread of multidrug-resistant (MDR) [1,2]. Thus, studies for the identification of novel targets and drugs for the treatment of infectious diseases are at the forefront. Several approaches to negating antibiotic resistance are currently being investigated, including inactivation of enzymes in essential metabolic pathways and inhibiting signal transduction systems [3,4]. These approaches involve the development of new antimicrobial drugs with modes of action that circumvent current resistance mechanisms [5,6].

Most of the platinum-based anticancer drugs [7] had an enormous impact on current cancer chemotherapy. However, the spectrum of cancer that can be treated with platinum agents is narrow and treatment efficacy suffers from side effects and resistance phenomena [8,9]. In order to overcome clinical problems associated with the relatively limited activity of platinum-based agents against the broad spectrum of human malignancies, acquired resistance and side effects, novel non-platinum metal-based anticancer complexes have been developed [9,10].

Notably, metallo-saldach compounds are very well-studied class of chemical nucleases that bind, cleave, and damage nucleic acids [11,12] via oxidative alkylation of nucleobases [13]. Furthermore, various Fe(III)-saldach derivatives have been implicated in efficient asymmetric catalysis and in catalyzing the hydrolytic cleavage of DNA and RNA [14]. Recent studies have demonstrated that Fe(III)-saldach induces apoptosis in human embryonic kidney cells [15]. Moreover, the *in vitro* DNA cleavage activity of Fe(III)-salen complexes is inversely correlated with their apoptotic activities in cultured human cells [16]. Mn(III)-saldach complexes were shown to exhibit superoxide dismutase (SOD), catalase activity and are considered to be synthetic SOD mimics [17,18]. Also Mn(III)-saldach induces tumor selective apoptosis in human cells [19].

In the race to synthesize new pharmaceutical drugs, ionic liquids (ILs) have attracted a great deal of attention. IL strategies can take advantage of the dual nature (discrete ions) of ILs to realize enhancements which may include controlled solubility, bioavailability or bioactivity, stability, elimination of polymorphism, new delivery options (e.g., slow release or the IL-API as 'solvent'), or even customized pharmaceutical cocktails [20]. 1,3-Dialkylimidazolium salts have become an attractive candidates for application in medicinal chemistry due to their tunable properties and ability to generate biological responses upon binding to several

* Corresponding authors at: Institut für Anorganische Chemie und Strukturchemie, Heinrich-Heine Universität Düsseldorf, 40204 Düsseldorf, Germany. Tel.: +20 1228123965.
E-mail addresses: reda_elshaarawi@science.suez.edu.eg, Reda.El-Shaarawy@uni-duesseldorf.de (R.F.M. Elshaarawy), kheiralla@hotmail.com (Z.H. Kheiralla), janiak@uni-duesseldorf.de (C. Janiak).

http://dx.doi.org/10.1016/j.ica.2014.05.029
0020-1693/© 2014 Elsevier B.V. All rights reserved.

biological targets [21]. They have been recognized as bactericidal [22], fungicidal [22], acetylcholinesterase (AChE) inhibitor [23], AMP deaminase inhibitor [24], delivery of anti-inflammatory drugs [25], local anesthetic [22], anti-nociceptive [20], anticholinergic [20], anticancer drugs [26] and in protein formulations [27]. Carson et al. have reported the broad spectrum antibiofilm activity of 1-alkyl-3-methylimidazolium chloride ILs against a panel of clinically important microbes [28]. Recently, the anti-microbial effect of a series of imidazolium-based ionic liquids revealed broad-spectrum activities against *cocci*, *rods* and *fungi* [29]. Also the length of *N*-3 alkyl substituent plays a significant role in the anti-tumor activity. Noteworthy, imidazolium units can slowly interact with the C=N or C≡N module, through electrophilic-nucleophilic interaction, leading to the fragmentation of the molecule [30].

In continuation of our ongoing programs directed toward the development of novel, potent, selective and less toxic therapeutic agents [31], we now report a concise, practical synthetic route and *in vitro* biological (antimicrobial and anticancer) evaluation of new saldach-bis(imidazolium) salts and their metal complexes (Scheme 1) which may allow us to develop a promising therapeutic strategy to combat antibiotic resistance and offer potent cytotoxic agents.

2. Materials and methods

Melting points were measured using a BÜCHI Melting point B-540 apparatus; all melting points were measured in open glass capillaries and are uncorrected. Elemental analyses for C, H, N, were performed with a Perkin-Elmer 263 elemental analyzer. FT-IR spectra were recorded on a BRUKER Tensor-37 FT-IR spectrophotometer in the range 400–4000 cm^{-1} as KBr disc in the 4000–550 cm^{-1} region with 2 cm^{-1} resolution or with an ATR (attenuated total reflection) unit (Platinum ATR-QL, diamond). For signal intensities the following abbreviations were used: br (broad), sh (sharp), w (weak), m (medium), s (strong), vs (very strong). UV/Vis spectra were measured at 25 °C in ethanol (10^{-5} mol/L) on a Shimadzu UV-2450 spectrophotometer using quartz cuvettes (1 cm). NMR-spectra were obtained with a Bruker Avance DRX200 (200 MHz for ^{1}H) or Bruker Avance DRX500 (125, 202 and 470 MHz for ^{13}C, ^{31}P and ^{19}F respectively) spectrometer with calibration to the residual proton solvent signal in DMSO-d_6 (^{1}H NMR: 2.52 ppm, ^{13}C NMR: 39.5 ppm), $CDCl_3$ (^{1}H NMR: 7.26 ppm, ^{13}C NMR: 77.16 ppm) against TMS ($\delta = 0.00$ ppm) for ^{1}H and ^{13}C, 85% phosphoric acid ($\delta = 0.00$ ppm) for ^{31}P and $CFCl_3$ ($\delta = 0.00$ ppm) for ^{19}F NMR. Multiplicities of the signals were specified s (singlet), d (doublet), t (triplet), q (quartet) or m (multiplet). The mass spectra of the synthesized saldach-bis(imidazolium) salts and their metal complexes were acquired in the linear mode for positive ions on a UHR-QTOF maXis 4G (Bruker Daltonics) and Bruker Ultraflex MALDI-TOF instrument equipped with a 337 nm nitrogen laser pulsing at a repetition rate of 10 Hz. The 2+ charge assignment of ions in HR-ESI-MS was confirmed by the $m/z = 0.5$ difference between the isotope peaks ($x, x+1, x+2$). The MALDI matrix material (1,8-dihydroxy-9(10H)-anthracenone (dithranol, DIT, $^{12}C_{14}H_{10}O_3$, $M = 226.077$ g/mol) was dissolved in chloroform at a concentration of 10 mg/mL. MALDI probes were prepared by mixing compound solution (1 mg/mL in CH_2Cl_2) with the matrix solution (1:10, v/v) in a 0.5 mL Eppendorf® micro tube. Finally 0.5 μL of this mixture was deposited on the sample plate, dried at room temperature and then analyzed. Peaks with chlorine showed the isotope ratio $^{35/37}Cl = 75.8:24.2$. Manganese (^{55}Mn 54.938 Da, 100%) or iron (^{56}Fe 55.934 Da, 91.2%) are either isotope pure or with a predominant isotope (^{54}Fe 53.939, 5.8%; ^{57}Fe 56.935 Da, 2.1%). For the mass spectral assignment: Peaks are based on ^{12}C with 12.0000 Da, ^{35}Cl with 34.968 Da, ^{55}Mn 54.938 Da, ^{56}Fe 55.934. dithranol, DIT, $^{12}C_{14}H_{10}O_3$, $M = 226.077$ g/mol $C_{38}H_{52}N_6O_2$ = [**4**–2 anions]$^{2+}$ = 624.45 $C_{38}H_{50}N_6O_2$ = [**4**–2H^+–2 anions]^0 = 622.44 $Me_2Im = C_5H_8N_2 = 96.078$ $Me_2ImH = C_5H_9N_2 = 97.086$ $C_{38}H_{50}N_6O_2FeCl = 713.3$. The molar conductances of 10^{-3} mol/L solution of various salts have been measured at ambient temperature with a digital conductivity meter (S30 SevenEasy™ conductivity, Mettler-Toledo Electronics, LLC, Polaris Parkway, Columbus). The overall accuracy of the conductance measurements was found to be ±0.2%. Magnetic measurements

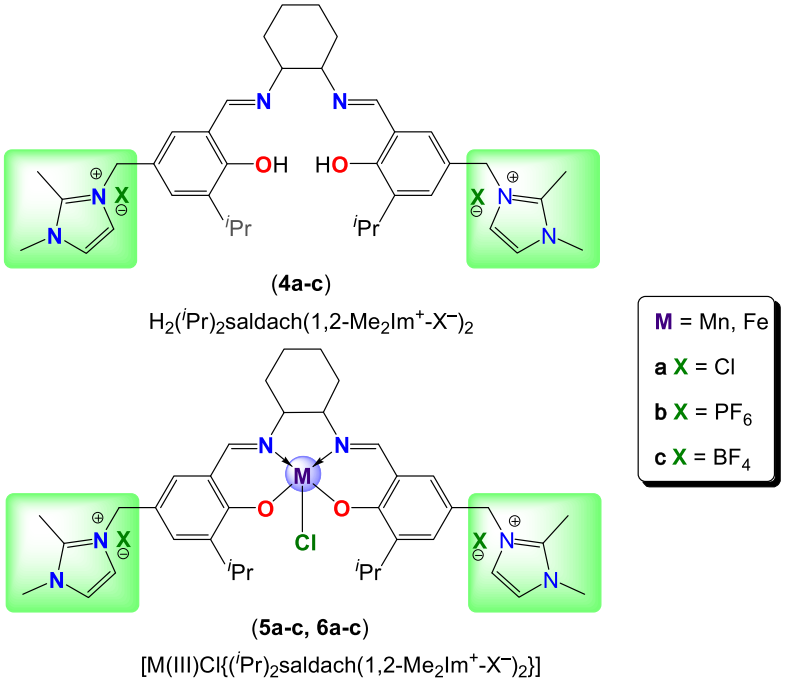

Scheme 1. $H_2(^{i}Pr)_2$saldach-bis(imidazolium) salts and chlorido-metal derivatives [M(III)Cl{($^{i}Pr)_2$saldach(1,2-Me_2Im^+-$X^-)_2$}] used in this work (saldach = *N*,*N*′-bis(salicylidene)-(±)-*trans*-1,2-diamino-cyclohexane).

of target complexes were carried out at room temperature using a Vibrating Sample Magnetometer (VSM), (Model PAR 155).

Chemicals were obtained from the following suppliers and used without further purification: salicylaldehyde, 2-*iso*-propylphenol, (±)-trans-1,2-diaminocyclohexane, anhydrous $MgCl_2$ and $Mn(CH_3COO)_2{\cdot}4H_2O$ (Sigma–Aldrich), paraformaldehyde (Roth), 1,2-dimethylimidazole, 1-butylimidazole (Alfa Aesar), triethylamine (Et_3N) and anhydrous $ZnCl_2$ (Grüssing GmbH) and $FeCl_3$ (Acros).

3. Experimental

The preparation details of the key starting materials 3-isopropylsalicylaldehyde (**1**), 3-iso-propyl-5-chloromethyl-2-hydroxybenzaldehyde (**2**), 3-(3-(iso-propyl)-5-formyl-4-hydroxybenzyl)-1,2-dimethylimidazol-3-ium chloride (**3**a) and anion metathesis products (**3**b,c) can be seen in electronic Supplementary information.

3.1. General procedure for the preparation of rac-trans-$H_2(^iPr)_2$saldach(1,2-Me_2Im^+-$X^-)_2$ (**4**a–c)

A methanolic solution (10 mL) of (±)-*trans*-1,2-diaminocyclohexane (dach) (0.23 g, 2.0 mmol) in a Schlenk tube, was added dropwise to a methanolic solution (20 mL) of salicylaldehyde-imidazolium salt H(^{i}Pr)sal(Me_2Im^+-X^-) **3**a–c (4.0 mmol) into a 100 mL Schlenk flask under nitrogen atmosphere. The reaction mixture was stirred under N_2 at 60 °C for 3 h. Then the solvent was partially removed under reduced pressure, and the yellow products of **4**a–c were precipitated by the addition of ethyl acetate and kept in the refrigerator overnight. Solvent was decanted off and the obtained crude product was sonicated for 15 min in Et_2O (3 × 25 mL). Et_2O was also decanted off and the residual solid was washed intensively with MeOH/Et_2O mixture (1:2) to remove unreacted materials and then re-dissolved in MeOH. EtOAc was added slowly (~15 min) to precipitate the products as pale yellow-dark orange solids which were collected by filtration and dried under vacuum. Samples of the isolated solids were characterized as follows.

3.1.1. N,N′-Bis[3-iso-propyl-5-((1,2-dimethylimidazol-3-ium)methylene)-salicylidene)-rac-trans-1,2-cyclohexanediamine dichloride monohydrate (**4**a)

Yellow-orange powder, (2.54 g, 89%); mp 61–63 °C. FT-IR (KBr, cm^{-1}): 3436 (m, br, $\nu_{(O-H)}$), 3131 (m, sh, $\nu_{asym(C-H)}$, Im and Ar), 3074 (m, sh, $\nu_{sym(C-H)}$, Im and Ar), 2931 (m, sh, $\nu_{(CH_3)}$ 2862 (m, sh, $\nu_{(C-H)}$), 1629 (vs sh, $\nu_{(C=N)}$), 1536, 1460, 1384 (s, sh, $\nu_{(C=C_{Ar}+C-H_{bend})}$, 1321 (m, sh, $\nu_{(C-H)}$), 1271 (s, sh, $\nu_{(Ar-O)}$), 1163 (s, sh, $\nu_{(H-C=C+H-C=N)_{bend}}$, Im), 770 (m, sh), 645 (m, sh), 505 (m, br). ^{1}H NMR (200 MHz, $CDCl_3$) δ (ppm): 13.98 (s, 2 H, 2 × Ar-O**H**), 8.55 (s, 2 H, 2 × **H**-C=N), 7.77 (d, J = 2.00 Hz, 2 H, 2 × Im-**H**), 7.72 (d, J = 1.97 Hz, 2 H, 2 × Im-**H**), 7.39 (d, J = 1.55 Hz, 2 H, 2 × Ar-**H**), 7.25 (d, J = 1.83 Hz, 2 H, 2 × Ar-**H**), 5.33 (s, 4 H, 2 × N(3)–C**H$_2$**–Ar), 3.77 (s, 6 H, 2 × N(1)–C**H$_3$**), 3.40 (m, 2 H, 2 × Cyhex-**H**), 3.22 ($m_{(7)}$, 2 H, 2 × C**H**$(CH_3)_2$), 2.64 (s, 6 H, 2 × C(2)–C**H$_3$**), 1.80 (m, 4 H, 4 × Cyhex-**H**), 1.49 (m, 4 H, 4 × Cyhex-**H**), 1.16 (d, J = 7.89 Hz, 12 H, 2 × CH(C**H$_3$**)$_2$). ^{13}C NMR (125 MHz, $CDCl_3$) δ (ppm): 165.23 (H**C**=N), 159.99 (**C**-OH), 144.58 (N(1)**C**(CH_3)N(3)), 137.67 (**C**, Ar), 129.88 (**C**H, Ar), 123.79 (**C**H, Ar), 122.89 (N(1)CH**C**HN(3)), 121.16 (N(1)**C**HCHN(3)), 117.99 (**C**-C=N), 71.03 (**C**H, Cyhex), 50.57 (N(3)–**C**H_2–Ar), 35.09 (N(1)–**C**H_3), 34.83 (**C**H_2, Cyhex), 32.87 (**C**H$(CH_3)_2$), 29.37 (CH(**C**$H_3)_2$), 24.12 (**C**H_2, Cyhex), 9.79 (C(2)–**C**H_3). ESI MS: m/z 624.4 (<5%, $[C_{38}H_{52}N_6O_2]^{+\cdot}$ = $[M-2Cl^-+e^-]^{+\cdot}$), 431.3 (20%, $[C_{38}H_{52}N_6O_2-Me_2ImH^+-Me_2Im]^+$), 312.2 (50%, $[C_{38}H_{52}N_6O_2]^{2+}$), 264.2 (100%, $[C_{38}H_{52}N_6O_2-Me_2Im]^{2+}$), 208.5 (45%, $[C_{38}H_{52}N_6O_2-Me_2ImH-Me_2ImCH_2]^{2+}$). *Anal.* Calc. for $C_{38}H_{52}Cl_2N_6O_2{\cdot}H_2O$ (M = 713.80): C, 63.94; H, 7.63; N, 11.77. Found: C, 63.83; H, 7.83; N, 11.49%.

3.1.2. N,N′-Bis-[3-iso-propyl-5-((1,2-dimethylimidazol-3-ium)methylene)-salicylidene)-rac-trans-1,2-cyclohexanediamine bis-(hexafluorophosphate) monohydrate (**4**b)

Yellow powder, (3.39 g, 91%); mp 84–85 °C. FT-IR (KBr, cm^{-1}): 3438 (m, br, $\nu_{(O-H)}$), 3181 (m, sh, $\nu_{asym(C-H)}$, Im and Ar), 3154 (m, sh, $\nu_{sym(C-H)}$, Im and Ar), 2938 (m, sh, $\nu_{(CH_3)}$) 2869 (m, sh, $\nu_{(C-H)}$), 1633 (vs sh, $\nu_{(C=N)}$), 1539, 1466, 1389 (s, sh, $\nu_{(C=C_{Ar}+C-H_{bend})}$), 1324 (m, sh, $\nu_{(C-H)}$), 1273 (s, sh, $\nu_{(Ar-O)}$), 1160 (s, sh, $\nu_{(H-C=C+H-C=N)_{bend}}$, Im), 838 (vs sh, $\nu_{(PF_6^-)_{str}}$), 774 (m, sh), 676 (m, sh), 557 (s, sh, $\delta_{(P-F)}$). ^{1}H NMR (200 MHz, DMSO-d_6) δ (ppm): 13.98 (s, 2 H, 2 × Ar-O**H**), 8.53 (s, 2 H, 2 × **H**-C=N), 7.66 (d, J = 2.12 Hz, 2 H, 2 × Im-**H**), 7.62 (d, J = 2.02 Hz,, 2 H, 2 × Im-**H**), 7.35 (d, J = 1.99 Hz, 2 H, 2 × Ar-**H**), 7.21 (d, J = 2.21 Hz, 2 H, 2 × Ar-**H**), 5.27 (s, 4 H, 2 × N(3)–C**H$_2$**–Ar), 3.75 (s, 6 H, 2 × N(1)–C**H$_3$**), 3.51 (s, br, 2 H, 2 × Cyhex-**H**), 3.22 ($m_{(7)}$, 2 H, 2 × C**H**$(CH_3)_2$), 2.61 (s, 6 H, 2 × C(2)–C**H$_3$**), 1.83 (m, 4 H, 4 × Cyhex-**H**), 1.55 (m, 4 H, 4 × Cyhex-**H**), 1.34 (dd, 12 H, J_1 = 1.62 Hz, J_2 = 6.93 Hz, 2 × CH(C**H$_3$**)$_2$). ^{13}C NMR (125 MHz, DMSO-d_6) δ (ppm): 165.96 (H**C**=N), 160.11 (**C**-OH), 144.68 (N(1)**C**(CH_3)N(3)), 137.68 (**C**, Ar), 129.94 (**C**H, Ar), 123.90 (**C**H, Ar), 122.91 (N(1)CH**C**HN(3)), 121.19 (N(1)**C**HCHN(3)), 118.51 (**C**—C=N), 71.14 (**C**H, Cyhex), 50.64 (N(3)–**C**H_2–Ar), 35.12 (N(1)–**C**H_3), 32.91 (**C**H_2, Cyhex), 29.38 (**C**H$(CH_3)_2$), 26.73 (CH(**C**$H_3)_2$), 24.07 (**C**H_2, Cyhex), 9.81 (C(2)–**C**H_3) (see Fig. S1 in Supplementary data). ^{31}P NMR (202 MHz, DMSO-d_6): −142.97 ppm (septet, $^2J_{PF}$ = 711.24 Hz). ^{19}F NMR (470 MHz, DMSO-d_6): −70.58 ppm (doublet, $^1J_{FP}$ = 715.68 Hz) (see Fig. S2 in Supplementary data). HR-ESI-MS: 527.3376 (<5%, $[C_{38}H_{52}N_6O_2-Me_2ImH\cdot]^+$), 431.2691 (25%, $[C_{28}H_{35}N_2O_2]^+$ = $[C_{38}H_{52}N_6O_2-Me_2ImH^+-Me_2Im]^+$), 312.2074 (100%, $[C_{38}H_{52}N_6O_2]^{2+}$), 264.1729 (60%, $[C_{33}H_{44}N_4O_2]^{2+}$ = $[C_{38}H_{52}N_6O_2-Me_2Im]^{2+}$), 208.47409 (10%, $[C_{38}H_{52}N_6O_2-Me_2ImH-Me_2ImCH_2]^{2+}$). MALDI-TOF MS, m/z: 849.4 [M+DIT−H^+−2 PF_6^-]$^+$, 769.4 (<10%, [M−PF_6^-]$^+$), 657.3 (40%, $[C_{38}H_{52}N_6O_2$+DIT−Me_2ImH^+−$Me_2Im]^+$), 431.2 (75%, $[C_{38}H_{52}N_6O_2-Me_2ImH^+-Me_2Im]^+$), 227.0 (100%, [DIT+$H^+$]$^+$). *Anal.* Calc. for $C_{38}H_{52}F_{12}N_6O_2P_2{\cdot}H_2O$ (M = 932.80): C, 48.93; H, 5.83; N, 9.01. Found: C, 49.14; H, 5.75; N, 9.20%.

3.1.3. Rac-trans-N,N′-Bis-[3-iso-propyl-5-((1,2-dimethylimidazol-3-ium)methylene)-salicylidene)- rac-trans-1,2-cyclohexanediamine bis-(tetrafluoroborate) monohydrate (**4**c)

Pale yellow powder, (3.04 g, 93%); mp 76–78 °C. FT-IR (KBr, cm^{-1}): 3441 (m, br, $\nu_{(O-H)}$), 3183 (m, sh, $\nu_{asym(C-H)}$, Im and Ar), 3151 (m, sh, $\nu_{sym(C-H)}$, Im and Ar), 2936 (m, sh, $\nu_{(CH_3)}$) 2867 (m, sh, $\nu_{(C-H)}$), 1632 (vs sh, $\nu_{(C=N)}$), 1539, 1466, 1388 (s, sh, $\nu_{(C=C_{Ar}+C-H_{bend})}$), 1324 (m, sh, $\nu_{(C-H)}$), 1274 (s, sh, $\nu_{(Ar-O)}$), 1159 (s, sh, $\nu_{(H-C=C+H-C=N)_{bend}}$, Im), 1060 (vs sh, $\nu_{(BF_4^-)_{str}}$), 865 (m, sh), 771 (m, sh), 678 (m, sh). ^{1}H NMR (200 MHz, DMSO-d_6) δ (ppm): 13.98 (s, 2 H, 2 × Ar-O**H**), 8.54 (s, 2 H, 2 × **H**-C=N), 7.66 (d, J = 2.08 Hz, 2 H, 2 × Im-**H**), 7.62 (d, J = 2.05 Hz, 2 H, 2 × Im-**H**), 7.36 (d, J = 1.96 Hz, 2 H, 2 × Ar-**H**), 7.22 (d, J = 2.08 Hz, 2 H, 2 × Ar-**H**), 5.27 (s, 4 H, 2 × N(3)–C**H$_2$**–Ar), 3.75 (s, 6 H, 2 × N(1)–C**H$_3$**), 3.52 (s, br, 2 H, 2 × Cyhex-**H**), 3.22 ($m_{(7)}$, 2 H, 2 × C**H**$(CH_3)_2$), 2.61 (s, 6H, 2 × C(2)-C**H$_3$**), 1.82 (m, 4 H, 4 × Cyhex-**H**), 1.50 (m, 4 H, 4 × Cyhex-**H**), 1.17 (dd, J_2 = 6.87 Hz, J_1 = 1.32 Hz, 12 H, 2 × CH(C**H$_3$**)$_2$). ^{13}C NMR (125 MHz, DMSO-d_6) δ (ppm): 165.59 (H**C**=N), 158.77 (**C**-OH), 144.70 (N(1)**C**(CH_3)N(3)), 136.53 (**C**, Ar), 129.36 (**C**H, Ar), 124.52 (**C**H, Ar), 122.91 (N(1)CH**C**HN(3)), 121.20 (N(1)**C**HCHN(3)), 118.07 (**C**—C=N), 71.44 (**C**H, Cyhex), 50.61 (N(3)–**C**H_2–Ar), 35.13 (N(1)–**C**H_3), 33.13 (**C**H_2, Cyhex), 26.41 (**C**H$(CH_3)_2$), 24.41 (CH(**C**$H_3)_2$), 22.67 (**C**H_2, Cyhex), 9.84 (C(2)–**C**H_3) (see Fig. S4 in Supplementary data). ^{19}F NMR (470 MHz, DMSO-

d_6): −148.72 ppm (singlet) (see Fig. S5 in Supplementary data). MALDI-TOF MS, *m/z*: 849.5 (10%, [M+DIT−H$^+$−2 BF_4^-]$^+$), 711.4 (25%, [M−BF_4^-]$^+$), 657.4 (60%, [$C_{38}H_{52}N_6O_2$+DIT−Me_2ImH^+−Me_2-Im]$^+$), 431.3 (100%, [$C_{38}H_{52}N_6O_2$−Me_2ImH^+−Me_2Im]$^+$), 227.0 (90%, [DIT+H$^+$]$^+$). *Anal.* Calc. for $C_{38}H_{52}B_2F_8N_6O_2$ H_2O (*M* = 816.48): C, 55.90; H, 6.67; N, 10.29. Found: C, 56.29; H, 6.66; N, 10.35%.

3.2. General procedure for the preparation of chlorido-metallosaldach-bis-imidazolium complexes [M(III)Cl{(^{i}Pr)$_2$saldach(Me_2Im^+-X$^-$)$_2$}] (M = Mn, Fe) (**5**a–c, **6**a–c)

3.2.1. Synthesis of Mn(III) complexes (**5**a–c)

A yellow solution of the saldach-bis-imidazolium salts, H_2(^{i}Pr)$_2$-saldach(Me_2Im^+-X$^-$)$_2$ **4**a–c, (0.9 mmol) in ethanol (10 mL) was degassed for 15 min. An ethanolic solution (5 mL) of Mn(OAc)$_2$·4H_2O (269 mg, 1.1 mmol) was then added with the yellow solution turning dark brown immediately, and the reaction mixture was refluxed for 2 h under N_2. LiCl (69.9 mg, 1.65 mmol) was then added and the solution was refluxed for an additional 2 h under air bubbling through the solution. After evaporating the solvent under reduced pressure, the residue was re-dissolved in CH_2Cl_2 (3 ml), over-layered ethyl acetate (3 ml) and the mixture kept in a refrigerator overnight. The precipitated solid was filtered off and washed with ethyl acetate and diethyl ether. Recrystallization from CH_2Cl_2/*n*-hexane yielded pure [Mn(III)Cl{(^{i}Pr)$_2$saldach(Me_2Im^+-X$^-$)$_2$}] **5**a–c.

*3.2.1.1. Chlorido-trans-[[2,2′-][(1,2-cyclohexanediyl) bis(nitrilomethylidyne)] bis[4-((1,2-dimethyl- imidazolium)methylene-6-(^{i}Pr-phenolato)]-[N,N′,O,O′] manganese(III) dichloride sesquihydrate (**5**a·1.5H_2O).* Dark-brown powder (679 mg, 93%). FT-IR (KBr, cm^{-1}): 3434 (m, br, $\nu_{(O-H)}$, lattice water), 3132 (m, sh, $\nu_{asym(C-H)}$, Im and Ar), 2948 (m, sh, $\nu_{(CH_3)}$) 2864 (m, sh, $\nu_{(C-H)}$), 1620 (vs sh, $\nu_{(C=N)}$), 1547, 1439, 1387 (s, sh, $\nu_{(C=C_{Ar}+C-H_{bend})}$), 1332 (m, sh, $\nu_{(C-H)}$), 1280 (s, sh, $\nu_{(Ar-O)}$), 1179 (s, sh, $\nu_{(H-C=C+H-C=N)_{bend}}$, Im), 832 (m, sh), 761 (m, sh), 678 (m, sh), 575 (m, sh, $\nu_{(Mn-N)}$), 474 (w, br, $\nu_{(Mn-O)}$). MALDI-TOF MS, *m/z*: 849.5 (10%, [ligand **4**a+DIT−H$^+$−2 Cl$^-$]$^+$)$^+$, 710.3 (10%, [$C_{38}H_{50}N_6O_2Mn$+DIT−Me_2ImH^+-−Me_2Im]$^+$), 657.3 (30%, [$C_{38}H_{52}N_6O_2$+DIT−Me_2ImH^+−Me_2Im]$^+$), 520.2 (20%, [$C_{38}H_{50}N_6O_2MnCl$−2 Me_2Im]$^+$), 506.1 (5%, [Mn(DIT)$_2$-−H$^+$]$^+$, 431.3 (20%, [$C_{38}H_{52}N_6O_2$−Me_2ImH^+−Me_2Im]$^+$), 227.0 (100%, [DIT+H$^+$]$^+$). *Anal.* Calc. for $C_{38}H_{50}Cl_3MnN_6O_2$·1.5H_2O (M = 811.16): C, 56.27; H, 6.59; N, 10.36. Found: C, 56.16; H, 6.23; N, 10.29%. μ_{eff} = 4.86 μ_B.

*3.2.1.2. Chlorido-trans-[[2,2′-][(1,2-cyclohexanediyl) bis(nitrilomethylidyne)] bis[4-((1,2-dimethyl-imidazolium)methylene-6-(^{i}Pr-phenolato)]-[N,N′,O,O′] manganese(III) bis-(hexafluoro-phosphate) monohydrate (**5**b·H_2O).* Brown powder (835 mg, 91%). FT-IR (KBr, cm^{-1}): 3436 (m, br, $\nu_{(O-H)}$, lattice water), 3157 (m, sh, $\nu_{asym(C-H)}$, Im and Ar), 2956 (m, sh, $\nu_{(CH_3)}$) 2868 (m, sh, $\nu_{(C-H)}$), 1619 (vs sh, $\nu_{(C=N)}$), 1549, 1440, 1389 (s, sh, $\nu_{(C=C_{Ar}+C-H_{bend})}$), 1332 (m, sh, $\nu_{(C-H)}$), 1279 (s, sh, $\nu_{(Ar-O)}$), 1179 (s, sh, $\nu_{(H-C=C+H-C=N)_{bend}}$, Im), 840 (vs sh, $\nu_{(PF_6^-)_{str}}$), 840 (s, sh), 782 (m, sh), 740 (m, sh), 678 (m, sh), 573 (m, sh, $\nu_{(Mn-N)}$), 559 (m, sh, $\delta_{(P-F)}$), 473 (w, br, $\nu_{(Mn-O)}$). MALDI-TOF MS, *m/z*: ligand spectrum with 657.3 and 431.3; and 710.3 (5%, [$C_{38}H_{50}N_6O_2Mn$+DIT−Me_2ImH^+−Me_2Im]$^+$), 520.2 (10%, [$C_{38}H_{50}N_6O_2MnCl$−2 Me_2Im]$^+$), 506.0 (<5%, [Mn(DIT)$_2$−H$^+$]$^+$ 227.0 (100%, [DIT+H$^+$]$^+$). *Anal.* Calc. for $C_{38}H_{50}ClF_{12}MnN_6O_2P_2$·$H_2O$ (*M* = 1021.18): C, 44.69; H, 5.13; N, 8.23. Found: C, 44.55; H, 5.19; N, 8.20%. μ_{eff} = 4.96 μ_B.

*3.2.1.3. Chlorido-trans-[[2,2′-][(1,2-cyclohexanediyl) bis(nitrilomethylidyne)] bis[4-((1,2-dimethyl-imidazolium)methylene-6-(^{i}Pr-phenolato)]-[N,N′,O,O′] manganese(III) bis-(tetrafluoro-borate) sesquihydrate (**5**c·1.5H_2O).* Reddish-brown powder (724 mg, 88%). FT-IR (KBr, cm^{-1}): 3437 (m, br, $\nu_{(O-H)}$, lattice water), 3149 (m, sh, $\nu_{asym(C-H)}$, Im and Ar), 2958 (m, sh, $\nu_{(CH_3)}$) 2867 (m, sh, $\nu_{(C-H)}$), 1620 (vs sh, $\nu_{(C=N)}$), 1548, 1441, 1389 (s, sh, $\nu_{(C=C_{Ar}+C-H_{bend})}$), 1334 (m, sh, $\nu_{(C-H)}$), 1281 (s, sh, $\nu_{(Ar-O)}$), 1178 (s, sh, $\nu_{(H-C=C+H-C=N)_{bend}}$, Im), 1058 (vs sh, $\nu_{(BF_4^-)_{str}}$), 830 (m, sh), 779 (m, sh), 756 (m, sh), 679 (m, sh), 572 (m, sh, $\nu_{(Mn-N)}$), 471 (w, br, $\nu_{(Mn-O)}$). MALDI-TOF MS, *m/z*:ligand spectrum with 849.5, 657.4 and 431.3, and 710.3 (15%, [$C_{38}H_{50}N_6O_2Mn$+DIT−Me_2ImH^+−Me_2Im]$^+$), 520.2 (20%, [C_{38}-$H_{50}N_6O_2MnCl$−2 Me_2Im]$^+$), 506.0 (<5%, [Mn(DIT)$_2$−H$^+$]$^+$, 227.0 (100%, [DIT+H$^+$]$^+$). *Anal.* Calc. for $C_{38}H_{50}B_2ClF_8MnN_6O_2$·1.5$H_2O$ (*M* = 913.33): C, 49.94; H, 5.85; N, 9.20. Found: C, 49.63; H, 5.91; N, 9.44%. μ_{eff} = 4.91 μ_B.

3.2.2. Synthesis of Fe(III) complexes (**6**a–c)

A yellow solution of the saldach-bis(imidazolium) salts H_2(^{i}Pr)$_2$-saldach(Me_2Im^+-X$^-$)$_2$ **4**a–c (0.9 mmol) in ethanol (10 mL) was degassed for 15 min. An ethanolic solution (5 mL) of $FeCl_3$ (177 mg, 1.1 mmol) was then added with the yellow solution turning dark reddish-brown immediately, and the reaction mixture was refluxed for 2 h under N_2. Then, the solution was concentrated and the residue was kept in a refrigerator overnight. The precipitated solid was filtered off and washed with cold ethanol (2 × 3 mL) and diethyl ether (3 × 3 mL) to yield [Fe(III)Cl{(^{i}Pr)$_2$-saldach(Me_2Im^+-X$^-$)$_2$}] **6**a–c.

*3.2.2.1. Chlorido-trans-[[2,2′-][(1,2-cyclohexanediyl) bis(nitrilomethylidyne)] bis[4-((1,2-dimethyl- imidazolium)methylene-6-(^{i}Pr-phenolato)]-[N,N′,O,O′] iron(III) dichloride sesquihydrate (**6**a·1.5H_2O).* Reddish-brown powder (687 mg, 94%). FT-IR (KBr, cm^{-1}): 3429 (m, br, $\nu_{(O-H)}$, lattice water), 3137 (m, sh, $\nu_{asym(C-H)}$, Im and Ar), 2935 (m, sh, $\nu_{(CH_3)}$) 2865 (m, sh, $\nu_{(C-H)}$), 1613 (vs sh, $\nu_{(C=N)}$), 1549, 1449, 1388 (s, sh, $\nu_{(C=C_{Ar}+C-H_{bend})}$), 1334 (m, sh, $\nu_{(C-H)}$), 1278 (s, sh, $\nu_{(Ar-O)}$), 1177 (s, sh, $\nu_{(H-C=C+H-C=N)_{bend}}$, Im), 834 (m, sh), 745 (m, sh), 678 (m, sh), 570 (m, sh, $\nu_{(Fe-N)}$), 498 (w, br), 467 (m, sh, $\nu_{(Fe-O)}$). MALDI-TOF MS, *m/z*: 746.3 (10%, [$C_{38}H_{50}N_6O_2$-FeCl+DIT−Me_2ImH^+−Me_2Im]$^+$), 711.3 (60%, [$C_{38}H_{50}N_6O_2$-Fe+DIT−Me_2ImH^+−Me_2Im]$^+$), 552.2 (30%, [$C_{38}H_{50}N_6O_2FeCl$(OMe)−2 Me_2Im]$^+$, 521.2 (80%, [$C_{38}H_{50}N_6O_2FeCl$−2 Me_2Im]$^+$), 507.1 (20%, [Fe(DIT)$_2$−H$^+$]$^+$, 226.9 (100%, [DIT+H$^+$]$^+$). *Anal.* Calc. for $C_{38}H_{50}Cl_3$-FeN_6O_2·1.5H_2O (*M* = 812.07): C, 56.20; H, 6.58; N, 10.35. Found: C, 56.14; H, 6.42; N, 10.72%. μ_{eff} = 5.63 μ_B.

3.2.2.2. Chlorido-trans-[[2,2′-][(1,2-cyclohexanediyl) bis(nitrilomethylidyne)] bis[4-((1,2-dimethyl-imidazolium)methylene-6-(^{i}Pr-phenolato)]-[N,N′,O,O′] iron(III) bis-(hexafluorophosphate) monohydrate (6b·~2H_2O). Brown powder (842 mg, 90%). FT-IR (KBr, cm^{-1}): Dark-brown powder (556 mg, 93%). FT-IR (KBr, cm^{-1}): 3430 (m, br, $\nu_{(O-H)}$, lattice water), 3145 (m, sh, $\nu_{asym(C-H)}$, Im and Ar), 2954 (m, sh, $\nu_{(CH_3)}$) 2867 (m, sh, $\nu_{(C-H)}$), 1615 (vs sh, $\nu_{(C=N)}$), 1549, 1442, 1391 (s, sh, $\nu_{(C=C_{Ar}+C-H_{bend})}$), 1328 (m, sh, $\nu_{(C-H)}$), 1279 (s, sh, $\nu_{(Ar-O)}$), 1178 (s, sh, $\nu_{(H-C=C+H-C=N)_{bend}}$, Im), 842 (vs sh, $\nu_{(PF_6^-)_{str}}$), 780 (m, sh), 740 (m, sh), 680 (m, sh), 557 (m, sh, $\delta_{(P-F)}$), 572 (w, br, $\nu_{(Fe-N)}$), 471 (m, br, $\nu_{(Fe-O)}$). MALDI-TOF MS, *m/z*: 746.3 (<5%, [$C_{38}H_{50}N_6O_2FeCl$+DIT−Me_2ImH^+−Me_2Im]$^+$), 711.3 (45%, [$C_{38}H_{50}N_6$-O_2Fe+DIT−Me_2ImH^+−Me_2Im]$^+$), 521.2 (40%, [$C_{38}H_{50}N_6O_2FeCl$−2 Me_2Im]$^+$), 507.1 (20%, [Fe(DIT)$_2$ – H$^+$]$^+$, 227.0 (100%, [DIT+H$^+$]$^+$). *Anal.* Calc. for $C_{38}H_{50}ClF_{12}FeN_6O_2P_2$·~2$H_2O$ (*M* = 1040.10): C, 43.88; H, 5.23; N, 8.08. Found: C, 44.01; H, 5.20; N, 8.11%. μ_{eff} = 5.86 μ_B.

*3.2.2.3. Chlorido-trans-[[2,2'-][(1,2-cyclohexanediyl) bis(nitrilomethylidyne)] bis[4-((1,2-dimethyl-imidazolium)methylene-6-(ⁱPr-phenolato)]-[N,N',O,O'] iron(III) bis-(tetrafluoroborate) monohydrate (**6**c·H_2O).* Dark-red powder (816 mg, 89%). FT-IR (KBr, cm^{-1}): 3442 (m, br, $\nu_{(O-H)}$, lattice water), 3150 (m, sh, $\nu_{asym(C-H)}$, Im and Ar), 2938 (m, sh, $\nu_{(CH_3)}$) 2868 (m, sh, $\nu_{(C-H)}$), 1616 (vs sh, $\nu_{(C=N)}$), 1551, 1453, 1391 (s, sh, $\nu_{(C=C_{Ar}+C-H_{bend})}$), 1329 (m, sh, $\nu_{(C-H)}$), 1282 (s, sh, $\nu_{(Ar-O)}$), 1179 (s, sh, $\nu(H-C{=}C+H-C{=}N)_{bend}$, Im), 1060 (vs sh, $\nu_{(BF_4^-)_{str}}$), 834 (m, sh), 748 (m, sh), 678 (m, sh), 573 (m, sh, $\nu_{(Fe-N)}$), 497 (w, br), 467 (m, sh, $\nu_{(Fe-O)}$), 443 (w, br). MALDI-TOF MS, *m/z*: 711.3 (20%, $[C_{38}H_{50}N_6O_2Fe+DIT-Me_2ImH^+-Me_2Im]^+$), 521.2 (15%, $[C_{38}H_{50}N_6O_2FeCl-2\ Me_2Im]^+$), 507.1 (5%, $[Fe(DIT)_2-H^+]^+$, 227.0 (100%, $[DIT+H^+]^+$). *Anal.* Calc. for $C_{38}H_{50}B_2ClF_8FeN_6O_2\cdot H_2O$ (*M* = 905.77): C, 50.39; H, 5.79; N, 9.28. Found: C, 50.54; H, 5.78; N, 9.33%. μ_{eff} = 5.75 μ_B.

3.3. In vitro anticancer (cytotoxicity) activity

3.3.1. Reagents

Dimethylsulphoxide (DMSO), crystal violet and Trypan blue dye were purchased from Sigma Chemical Co. (St. Louis, Mo, USA). Dulbecco's modified Eagle's medium (DMEM), Roswell Park Memorial Institute medium (RPMI-1640), Fetal Bovine Serum (FBS), 4-(2-Hydroxyethyl)piperazine-1-ethanesulfonic acid (HEPES) buffer solution, L-glutamine, gentamycin and 0.25% Trypsin-EDTA were obtained from Lonza.

Crystal violet stain: prepared as 0.5% crystal violet solution by dissolving 0.5 g of crystal violet stain in 50 mL methanol, then the solution was completed to 100 mL with deionized water, filtered through Whatmann No. 1 and stored at room temperature.

3.3.2. Cell cultures

Two human tumor cell lines, MCF-7 (breast adenocarcinoma) and Hepg2 (liver hepatocellular carcinoma) were obtained from the VACSERA Tissue Culture Unit and cultured in either RPMI-1640 or DMEM media supplemented with 10% heat-inactivated FBS, 1% L-glutamine, HEPES buffer and 50 μg/mL gentamycin. All cells were maintained at 37 °C in a humidified atmosphere with 5% CO_2 and sub-cultured two times a week. Cell toxicity was monitored by determining the effect of the tested samples on cell morphology and cell viability. The effect of the vehicle solvent (DMSO) on the growth of these cell lines was evaluated in all the experiments by exposing untreated control cells to the maximum concentration (0.5%) of DMSO used in each assay.

3.3.3. Cytotoxicity assay

The *in vitro* cytotoxicity of the saldach-bis-imidazolium salts and their chlorido M(III) complexes were measured by the cytotoxic effect assay according to the procedure adopted by the Regional Center for Mycology & Biotechnology, Egypt. Briefly, the cells were seeded in 96-well plates at a cell concentration of 1×10^4 cells per well in 100 μL of growth medium. Fresh medium containing different concentrations of the tested sample was added after 24 h of seeding. Serial twofold dilutions of the tested compound were added to confluent cell mono layers dispensed into 96-well, flat-bottomed micro titer plates (Falcon, NJ, USA) using a multichannel pipette. The micro-titer plates were incubated at 37 °C in a humidified incubator with 5% CO_2 for a period of 48 h. Three wells were used for each sample concentration. Control cells were incubated without tested sample and with or without DMSO. The little percentage of DMSO present in the wells (maximal 0.1%) is not affecting the experiment. After incubation of the cells for 24 h at 37 °C, various concentrations of sample (1.50–70.04 μM) were added, and the incubation was continued for 48 h then the viable cells yield was determined by a colorimetric method. After the end of the incubation period, media were aspirated and the crystal violet solution (1%) was added to each well for at least 30 min. The stain was removed and the plates were rinsed using tap water until all excess stain was removed. Glacial acetic acid (30%) was then added to all wells and mixed thoroughly, and then the absorbance of the plates were measured after gently shaken on Micro plate reader (TECAN, Inc.), using a wavelength of 490 nm. All results were corrected for background absorbance detected in wells without stain. Treated samples were compared with the cell control in absence of the tested compounds. All experiments were carried out in triplicate and the average values were calculated. The cell cytotoxic effect of each tested compound was calculated [32].

3.4. Antibacterial survey

3.4.1. Reagents

Dimethylsulphoxide (DMSO) and Ampicillin antibiotic were obtained from Sigma Chemical Co. (St. Louis, MO, USA).

3.4.2. Bacterial cultures

Multi-drug resistant (MDR) strains used in this study from National Organization for Drug Control and Research (NODCAR), Cairo, Egypt. The different strains are *Staphylococcus aureus* (*S. aureus*, ATCC-29737), *Staphylococcus epidermidis* (*S. epidermidis*, ATCC-12228), *Streptococcus pneumoniae* and (*S. pneumoniae*, ATCC-49619) as representatives for the Gram-positive bacteria and *Escherichia coli* (*E. coli*, ATCC-10536), *Pseudomonas aeruginosa* (*P. aeruginosa*, ATCC-27853), *Shigella flexneri* (*S. flexneri*, ATCC-12022), *Klebsiella pneumonia* (*K. pneumonia*, ATCC-13883) and *Neisseria meningitidis* (*N. meningitidis*, ATCC-13090) as the most important Gram-negative pathogenic bacteria. Stock cultures grown aerobically on nutrient broth (NB) agar slants (Hi-Media) at 37 °C were maintained at 4 °C. Pre-cultures containing 10^5 CFU/ml, grown aerobically in Mueller Hinton (MH) liquid medium (Hi-Media) at 37 °C for 5 h, were used as inoculum for all experiments.

3.4.3. Bactericidal assay (antibacterial susceptibility testing)

Antibacterial susceptibility of the bacterial strains was carried out by agar well diffusion method [33] towards the most potent cytotoxic compounds (**4**a–c). As an indicator of antibacterial activity, the clear zone around the wells was measured as inhibition zones and the diameter of these zones of inhibition (ZOI, mm) were measured accurately using a transparent meter rule and recorded if the zone of inhibition was $\geqslant$10 mm [34]. Duplicates were maintained in each extract and the average values were calculated for the eventual antibacterial activity. Ampicillin, Antibacterial, was employed as standard drugs.

3.4.3.1. Determination of MIC and MBC. As a parameter of the antibacterial efficacy, the minimal inhibitory concentration (MIC) and minimal bactericidal concentration (MBC) of new compounds (**4**a–c) against Gram-positive and Gram-negative isolates were determined using the macro-dilution broth susceptibility test. Freshly prepared MH broth was used as diluents in the macro-dilution method. A serial dilution of each target compound was prepared within a desired range (0.12 mM to 28.02 mM). One milliliter of the Stock cultures was then inoculated and tubes were incubated at 37 °C for 24 h, control tubes without any addition were assayed simultaneously. MIC was examined visually, by checking the turbidity of the tubes. Furthermore the tubes having lesser concentration than MIC level were inoculated on MHA plate for MBC determination.

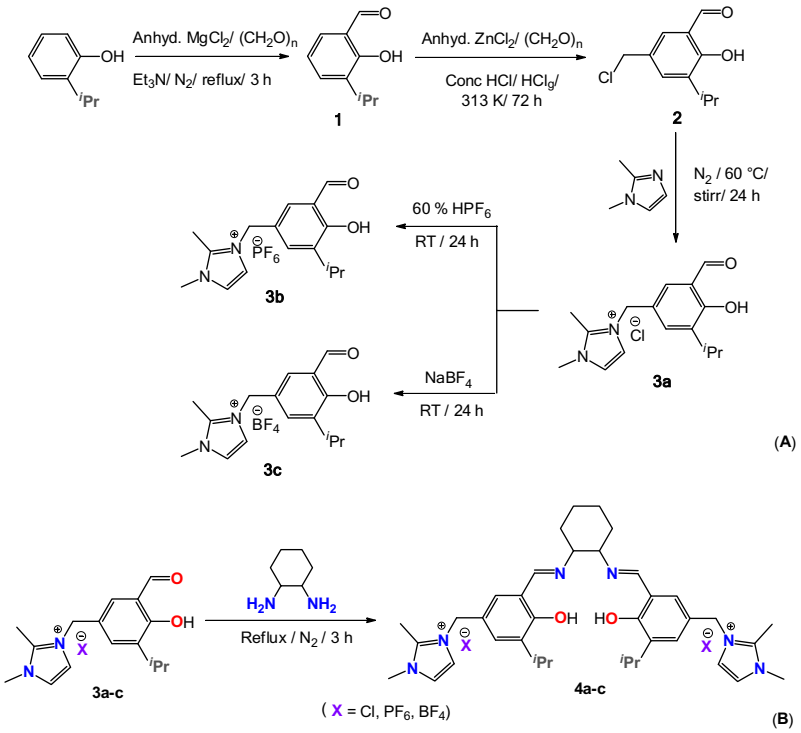

Scheme 2. Synthesis of: (A) salicylaldehyde salts [H(^{i}Pr)sal(Me_2Im^+-X^-)] (**3**a–c), (B) saldach-bis-(1,2-dimethylimidazolium) salts [*rac-trans*-(H_2(^{i}Pr)$_2$saldach-(Me_2Im^+-X^-)$_2$] (**4**a–c).

4. Results and discussion

4.1. Chemistry

4.1.1. Synthesis of rac-trans-(H_2(^{i}Pr)$_2$saldach(Me_2Im^+-X^-)$_2$) (X = Cl, **4***a*; PF_6, **4***b*; BF_4, **4***c*)

The synthesis of saldach-scaffold bearing bis-imidazolium terminal compartments **4**a–c is depicted in Scheme 2. The key starting materials salicylaldehyde-imidazolium salts **3**a–c were synthesized starting from 2-*iso*-propylphenol following modified literature procedures [35]. Under extra dry conditions and using anhydrous magnesium dichloride as O-magnesiation reagent, 2-*iso*-propylphenol was ortho-formylated by paraformaldehyde in the presence of catalytic amounts of triethylamine. 3-*iso*-Propylsalicylaldehyde was then chloromethylated to yield 5-chloromethyl-3-*iso*-propylsalicylaldehyde **2** in high purity (see Scheme 2A). Compound **2** allowed the preparation of a common precursor, **3**a, through the quarternization reaction of 1,2-dimethylimidazole with **2** to afford the salicylaldehyde-imidazolium chloride (**3**a). This salt was then readily metathesized into the corresponding hexafluorophosphate and tetrafluoroborate salts (**3**b,c) *via* reaction with aqueous hexafluorophosphoric acid, HPF_6(-aq), and sodium tetrafluoroborate, $NaBF_4$, respectively. The ligands, *rac-trans*-H_2(^{i}Pr)$_2$saldach(Me_2Im^+-X^-)$_2$ (**4**a–c), were synthesized by Schiff-base condensation reaction between compounds **3**a–c and (±)-*trans*-1,2-diaminocyclohexane (*rac-trans*-dach) in methanolic solution (see Scheme 2B). The *rac-trans*-configuration of the *N*,*N*′-bis(salicylidene)-1,2-cyclohexanediamine (saldach) backbone was selected, because metal–ligand binding will force the ligand to get a flat chair (planar) conformation, similar to the 1,2-cyclohexanediamine moiety present in oxaliplatin, a very promising metal-based drug [36]. Furthermore, the imine bond and salicyl effect lead to a very rigid configuration with only possible rotation around the N–C axis of diaminocyclohexane group. The saldach-bis(imidazolium) salts **4**a–c were isolated in high yields and characterized by FTIR, UV/Vis, ^{1}H NMR, ^{13}C NMR, ^{19}F NMR, ^{31}P NMR, ESI-MS, MALDI-TOF MS and conductivity measurements.

4.1.2. Synthesis of the metallosaldach-imidazolium salts [M(III)Cl{(^{i}Pr)$_2$saldach(Me_2Im^+-X^-)$_2$}] (M = Mn, **5**; Fe, **6**), (X = Cl, *a*; PF_6, *b*; BF_4, *c*)

A two-step one-pot preparative route (see Scheme 3) was used to prepare the chlorido Mn(III) complexes, [Mn(III)Cl{(^{i}Pr)$_2$saldach(Me_2Im^+-X^-)$_2$}] (X = Cl, PF_6, BF_4) (**5**a–c). This synthetic route involve exchange of acetate ligands in $Mn(OAc)_2{\cdot}4H_2O$ by (^{i}Pr)$_2$-saldach(Me_2Im^+-X^-)$_2$ under anaerobic conditions (N_2-atmosphere). Then spontaneous oxidation of Mn(II) center into Mn(III) species was allowed by molecular oxygen [37], followed by coordination of a chloride ion from lithium chloride (LiCl).

The Fe(III) complexes, [Fe(III)Cl{(^{i}Pr)$_2$saldach(Me_2Im^+-X^-)$_2$}] (X = Cl, PF_6, BF_4) (**6**a–c), were prepared by refluxing a solution of the corresponding saldach ligands, (H_2(^{i}Pr)$_2$saldach(Me_2Im^+-X^-)$_2$), with anhydrous Fe(III) chloride in methanol (UV-spectroscopy grade) under aerobic conditions (cf. Scheme 3).

Unfortunately all attempts to obtain X-ray diffraction quality single crystals of the Mn(III)- and Fe(III)-saldach-imidazolium chlorides ((**5**,**6**)a–c) were unsuccessful. Yet, the metal–ligand structures suggested in this work based upon elemental and spectral analysis (FTIR, UV–Vis, MALDI-TOF [38] conductivity as well as magnetic measurements and match with the structures of reported metal-saldach analogues (Table S1, Supplementary data).

4.2. Characterizations of the saldach-bis(imidazolium) salts and their complexes

4.2.1. Microanalytical data, conductivity and mass spectrometry

Saldach-bis(imidazolium) salts (**4**a–c) and their complexes were prepared in high yields, gave satisfactory C, H, and N elemental analyses, which are consistent with the proposed formula for the ligands and their chelate complexes (see the Section 3).

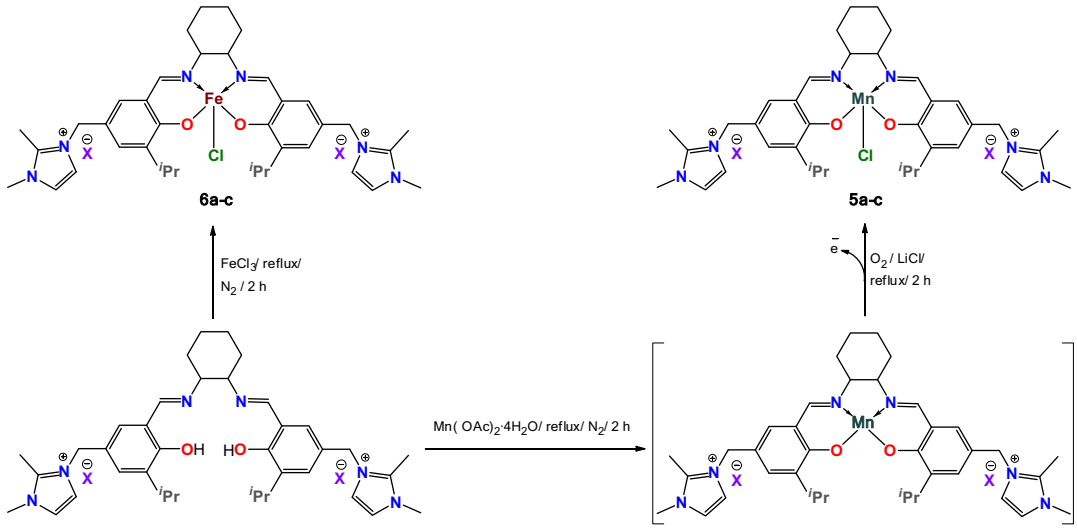

Scheme 3. Synthesis of metallosaldach-bis(imidazolium) complexes [M(III)Cl{*rac-trans*-(^{i}Pr)$_2$saldach-(Me_2Im^+-X^-)$_2$}] ((**5**,**6**)a–c).

Molar conductance values of all the saldach-bis(imidazolium) salts and their complexes in EtOH (1×10^{-3} M) at 25 °C are in the region of 49.1–84.5 and 51.3–95.0 μS/cm, respectively, in accordance with their ionic nature. The molar conductivities of the saldach-bis(imidazolium) salts H_2(^{i}Pr)$_2$saldach(Me_2Im^+-X^-)$_2$ decrease in the following order: **4**c (X = BF_4) > **4**a (X = Cl) > **4**b (X = PF_6).

The HR-ESI$^+$ mass spectra of **4**a and **4**b show dominant signals for the doubly-charged cation $[C_{38}H_{52}N_6O_2]^{2+}$ and species assuming both imidazolium groups have been lost, $[C_{38}H_{52}N_6O_2-Me_2ImH^+-Me_2Im]^+$ and $[C_{38}H_{52}N_6O_2-Me_2Im]^{2+}$.

The MALDI-TOF spectra of **4**b and **4**c display signals corresponding to the cation-(DIT–H$^+$)-matrix adduct [M+DIT−H$^+$−2 X_6^-]$^+$, the cation with one anion [M−X$^-$]$^+$, the cation where both imidazolium groups have been lost (with and without DIT) $[C_{38}H_{52}N_6O_2$+DIT−Me_2ImH^+−$Me_2Im]^+$ and $[C_{38}H_{52}N_6O_2-Me_2ImH^+-Me_2Im]^+$. The protonated DIT+H$^+$ matrix signal is usually the base peak. The DIT-matrix adduct ion is formed as a result of the intermolecular hydrogen bonding with the phenolic oxygen and π-π stacking of the aromatic rings [39].

In the metal complexes **5**,**6**a–c the metal-containing ions consist of metal–ligand species where both imidazolium groups have been lost, $[C_{38}H_{50}N_6O_2M$+DIT−Me_2ImH^+−$Me_2Im]^+$ and $[C_{38}H_{50}N_6O_2MCl$−2 $Me_2Im]^+$. Either the chlorido ligand is retained or replaced by a DIT ligand. Additionally, a signal for a metal-bis(DIT) complex, [M(DIT)$_2$−H$^+$]$^+$, is also observed. In the iron complexes **6**a,b also a signal for $[C_{38}H_{50}N_6O_2FeCl$+DIT−Me_2ImH^+−$Me_2Im]^+$ was detected. The protonated DIT+H$^+$ matrix signal is also the base peak in the MALDI-TOF-MS of the metal complexes.

4.2.2. IR spectroscopic data

The most informative evidence confirming the anchoring of central saldach backbone to the terminal imidazolium groups was obtained by FT-IR spectra. All saldach-bis(imidazolium) salts show a broad band at the range of 3436–3441 cm^{-1} attributed to the stretching vibration of the intramolecular hydrogen bonded phenolic OH group. All saldach-bis(imidazolium) salts contain two O–H···N intramolecular hydrogen bonds within the 2-hydroxybenzylidene-imine moieties (Scheme 4) which is further confirmed by the displacement of the azomethene (—HC=N—) stretching band of **4**a–c to lower wavenumber, *ca* 1631 cm^{-1}, compared with that of the free azomethene moiety [40,41]. Moreover, an additional band around 1271 was observed for the samples, which was assigned to the stretching vibration of Ar–O. The vibrational bands at ~865 and ~770 cm^{-1} are due to the in-plane and out-of plane flexible vibrations of the imidazolium ring.

The presence of the saldach-bis(imidazolium) salts as well as its binding mode within the complexes was assigned on the basis of vibrational spectroscopy. The general displacement of the $\nu_{(C=N)}$ bands to lower frequencies compared to that of the free ligands (Fig. 1) (see Table S2, Supplementary data) confirms the coordination of the azomethene nitrogen atom to the metal center [42].

The appearance of a new band in the spectra of complexes around 570 cm^{-1}, assigned to $\nu_{M(III)-N}$ vibrations (M = Mn, Fe) [43], is further support for this coordination. Strong bands attributable to phenolic oxygen $\nu_{(Ar-O)}$ undergo positive frequency shift, which is evidence for the ligation of the phenolate oxygen to metal ion, this is further confirmed by the appearance of a new band at 467–474 cm^{-1} which is assigned to the ν_{M-O} vibration. The presence of $\nu_{(O-H)}$ bands around 3430 cm^{-1} confirms the hydrate nature suggested by the analytical data for new complexes.

The IR spectral studies reveal that, the imine nitrogen atoms and phenolate oxygen atoms coordinate to a metal atom.

4.2.3. NMR studies and tautomerism scenario

We could identify the possible tautomeric equilibria with their relative tautomer population, in the saldach-bis-imdazolium salts **4**a–c by comparing with the NMR studies of the related salen and salophen Schiff base–based ligands (Scheme S1, Supplementary data) isolated in the former work [44,45] and salophen ligands [46]. These studies reveal that the central salen/salophen/saldach backbone is in the expected O-protonated (enol-imine) tautomeric form (cf. Scheme S1, Supplementary data). However, at first glance in the ^{1}H NMR spectrum of the ligand **4**a (Fig. 2) appear to be quite complicated. It exhibits two groups of signals due to a pair of tautomers with different populations, the neutral bis-(enolimine) with some contribution of the ionic phenolate-iminium resonance structure (cf. Scheme 4). Two singlets at 13.98 ppm, 2H, of phenolic O–H typical for bis-(enolimine) tautomer and at 13.56 ppm, 1H, for O–H of enolimine/phenolate-iminium tautomer. The NH resonance (8.55 ppm) is a singlet which is consistent with the structure of the bis-(enolimine) tautomer and a singlet/doublet set (8.62/8.43 ppm), this is agrees with enolimine/phenolate-iminium tautomer. Thus, ^{1}H NMR spectrum demonstrates that, in **4**a the central saldach backbone is in the enolimine form with some contribution

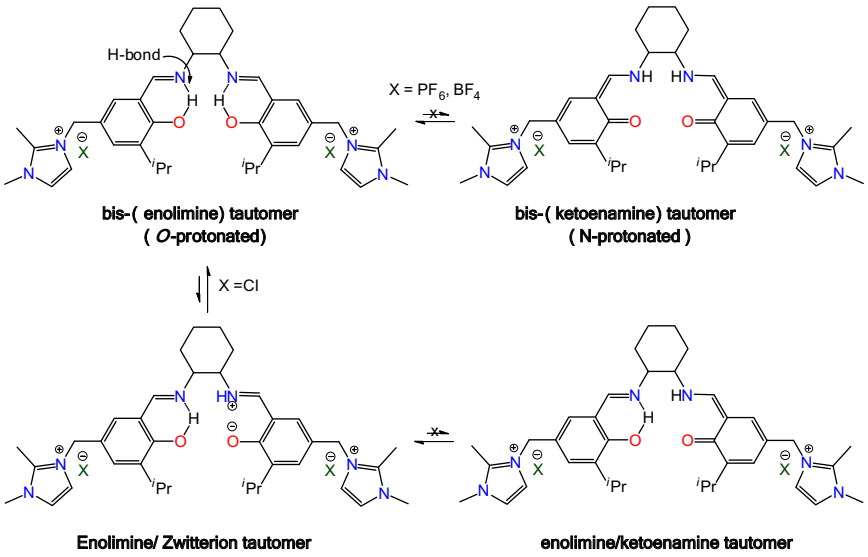

Scheme 4. Tautomeric equilibrium and hydrogen bonding in *rac-trans*-(H_2(^{i}Pr)$_2$saldach-(1,2-Me_2Im^+-X^-)$_2$ (X = PF_6, BF_4).

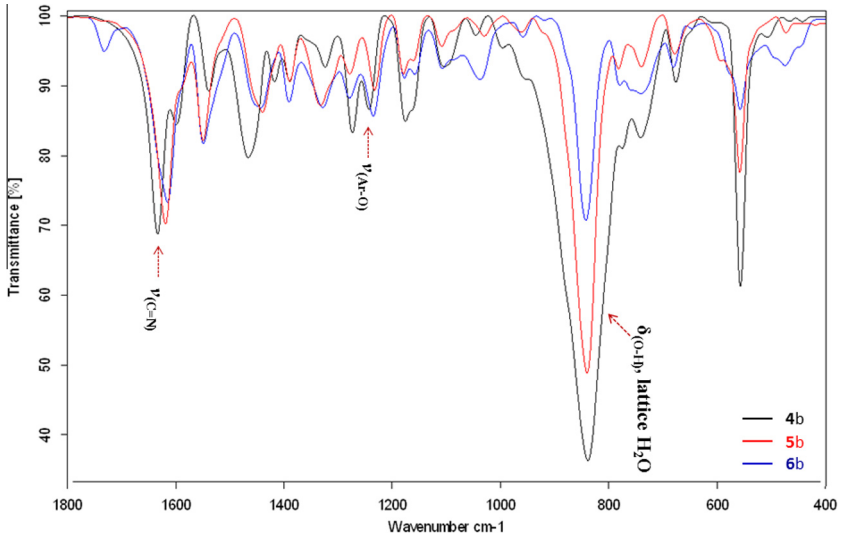

Fig. 1. Selected IR region, for comparison of the azomethine and phenolate stretching vibrations and their splitting patterns in **4**b, **5**b and **6**b.

of the enolimine/phenolate-iminium form in the solution (cf. Scheme 4).

Contrary, examination of the ^{1}H NMR spectra of H_2(^{i}Pr)$_2$saldach(1,2-Me_2Im^+-X^-)$_2$ (**4**b,c) (see Supplementary data) leads us to highlight the following aspects: (i) The singlets corresponding to the phenol OH and azomethine (H—C=N) protons are observed at 13.98 ppm (2H) and round 8.54 (2H), respectively. (ii) The central saldach backbone is in the *O*-protonated tautomeric form not in the *N*-protonated tautomeric form and the downfield shift of phenolic proton signal in all ligands as a result of the intramolecular H-bond to the imine nitrogen (cf Scheme 4). (iii) The phenyl, imidazolium, methylene, cyclohexyl, methyl and isopropyl protons are slight affected by anion metathesis, depending on the different arrangement adopted by the protons.

Further evidence for the *O*-protonated tautomer in both compartments is provided by ^{13}C NMR spectroscopy (see Supplementary data). Claramunt et al. remarked that the ^{13}C resonance varies from ~160 ppm for an enol-imine to ~180 ppm for a pure keto-enamine tautomer [47], making the ^{13}C resonance a powerful parameter to discern the relative tautomeric population. The ^{13}C NMR spectra of H_2(^{i}Pr)$_2$saldach(1,2-Me_2Im^+-X^-)$_2$ exhibits resonance at *ca* 160.0 ppm typical for enol-imines tautomer (160.9 ppm) [48]. Furthermore, signal around 166 ppm is observed, which can be assigned to the carbons of the aldimine (H—C=N) moieties [49]. Thus, NMR studies of **4**b,c reveal that, the acidic protons of the central saldach backbone are bond to O and not bond to N.

^{1}H–^{13}C COSY NMR (HMQC) experiments (Figs. S4, S8, Supplementary data) prove correlations between with the "imine" proton (**H**—C=N—Cyhex), which appears as a singlet (8.53 ppm for X = PF_6; 8.54 ppm for X = PF_6), and aldimine carbon (H—**C**=N—Cyhex), which appears at (165.96 ppm for X = PF_6; 166.00 ppm for X = PF_6). This correlation pattern has already been observed for the *O*-protonated ligands H_2(^{i}Pr)$_2$saldach(1,2-Me_2Im^+-X^-)$_2$ and was proposed for the pure *O*-protonated tautomer. These results demonstrate that the acidic protons are bond to oxygen only in solution.

4.2.4. Electronic absorption spectroscopy and magnetic susceptibility

In H_2(^{i}Pr)$_2$saldach(1,2-Me_2Im^+-X^-)$_2$ (**4**a–c) the absorption centered at *ca* 222 and 259 nm originate from the $\pi \rightarrow \pi^*$ and $n \rightarrow \pi^*$ transitions associated with the phenolic chromophor [50],

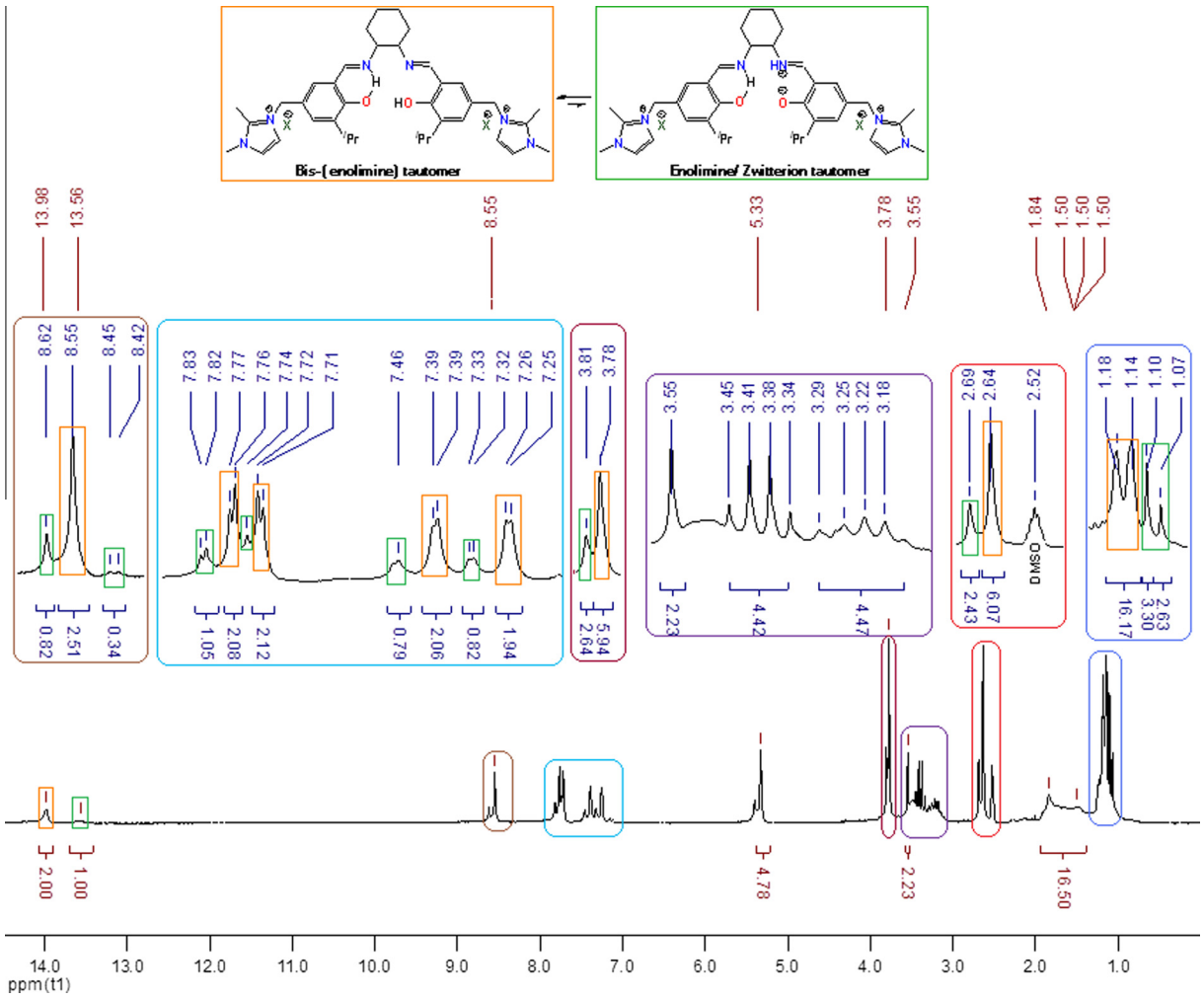

Fig. 2. ^{1}H NMR spectra of **4**a (200 MHz, DMSO-d_6).

while the peak at 325 nm can be assigned to the $\pi \rightarrow \pi^*$ transition involving the imine group [50], (see Fig. S16 in Supplementary data).

By going from the free saldach-bis-imdazolium salts to their mononuclear complexes [M(III)Cl{(^{i}Pr)$_2$saldach(Me$_2$Im$^+$-X$^-$)$_2$}] ((**5**,**6**)a–c), the UV/Vis spectra give further evidence for complexation where the characteristic bands of the neat saldach-bis-imdazolium salts are red-shifted (Table S3, Fig. S7–S10, Supplementary data). The most important feature in the near-UV region of the M(III)-saldach-imidazolium salts is the shift of the imine $\pi \rightarrow \pi^*$ transition band from 324 nm ($\varepsilon \times 10^3$ = 0.48–1.10 M^{-1}cm^{-1}) to higher wavelengths over 400 nm ($\varepsilon \times 10^3$ = 0.46–0.77 M^{-1}cm^{-1}) which indicates the coordination of metal ion with ligands [51]. In addition, the low intensity broad absorption round 500 nm ($\varepsilon \times 10^3$ = 0.09–0.84 M^{-1}cm^{-1}) which can be assigned to the three allowed d–d transitions expected for complexes with a square pyramidal geometry, ($d_{xz} \rightarrow d_{x^2-y^2}$), ($d_{xy} \rightarrow d_{x^2-y^2}$, d_{yz}) and ($d_z^2 \rightarrow d_{x^2-y^2}$) [52].

The magnetic moment values for the complexes (4.85–4.96 μ_B for Mn(III) saldach and 5.63–5.86 μ_B Fe(III) saldach) are also supportive of square pyramidal geometry with high spin metal centers [53].

4.3. Pharmacology

Many clinical trials of new active pharmaceutical ingredients (API) end in failure due to the low efficacy of the drug due to a limited bioavailability or solubility. With respect amphiphilicity, lipophilicity and solubility of imidazolium units, the anchoring of imidazolium compartments to the H$_2$(^{i}Pr)$_2$saldach provides a synergetic effect: it increases water solubility and at the same time enhances the pharmacological effect. Also the symmetric compounds, with two imidazolium units, are easier to synthesize than the unsymmetric ones, with one imidazolium unit.

4.3.1. In vitro cytotoxicity

The *in vitro* cytotoxicity of the saldach-bis(imdazolium) salts, H$_2$(^{i}Pr)$_2$saldach(1,2-Me$_2$Im$^+$-X$^-$)$_2$, **4**a–c as well as their metal complexes was evaluated in relation to the anticancer drug doxorubicin (C$_{27}$H$_{29}$NO$_{11}$, 543.52 g/mol) against human breast carcinoma (MCF-7) and human hepatocellular carcinoma (HepG2) cell lines (Tables S5, S6 Supplementary data). IC$_{50}$ values of the target compounds are in the range of 18.1–50.9 μg (Fig. 3, Table 1). The cell viability assays revealed that, all compounds had inhibitory effects on the growth of MCF-7 cell line more effectively than HepG2 cell line. Also H$_2$(^{i}Pr)$_2$saldach-(Me$_2$Im$^+$)$_2$X$^-$ (**4**a–c) are more effective in inducing cell death (cytotoxic) than their M(III)-complexes [M(III)Cl{(^{i}Pr)$_2$saldach(Me$_2$Im$^+$-X$^-$)$_2$}] ((**5**,**6**)a–c).

Noteworthy, the saldach-bis-imidazolium chloride, hexafluorophosphate and tetrafluoroborate (**4**a–c) showed different levels of cytotoxicity against MCF-7 cells where the tetrafluoroborate salt (**4**c) (IC$_{50}$ = 22.17 μM) is the most effective in inducing cell death and the chloride derivative (**4**a) (IC$_{50}$ = 33.34 μM) affect MCF-7 cell viability more than the hexafluorophosphate one (**4**b)

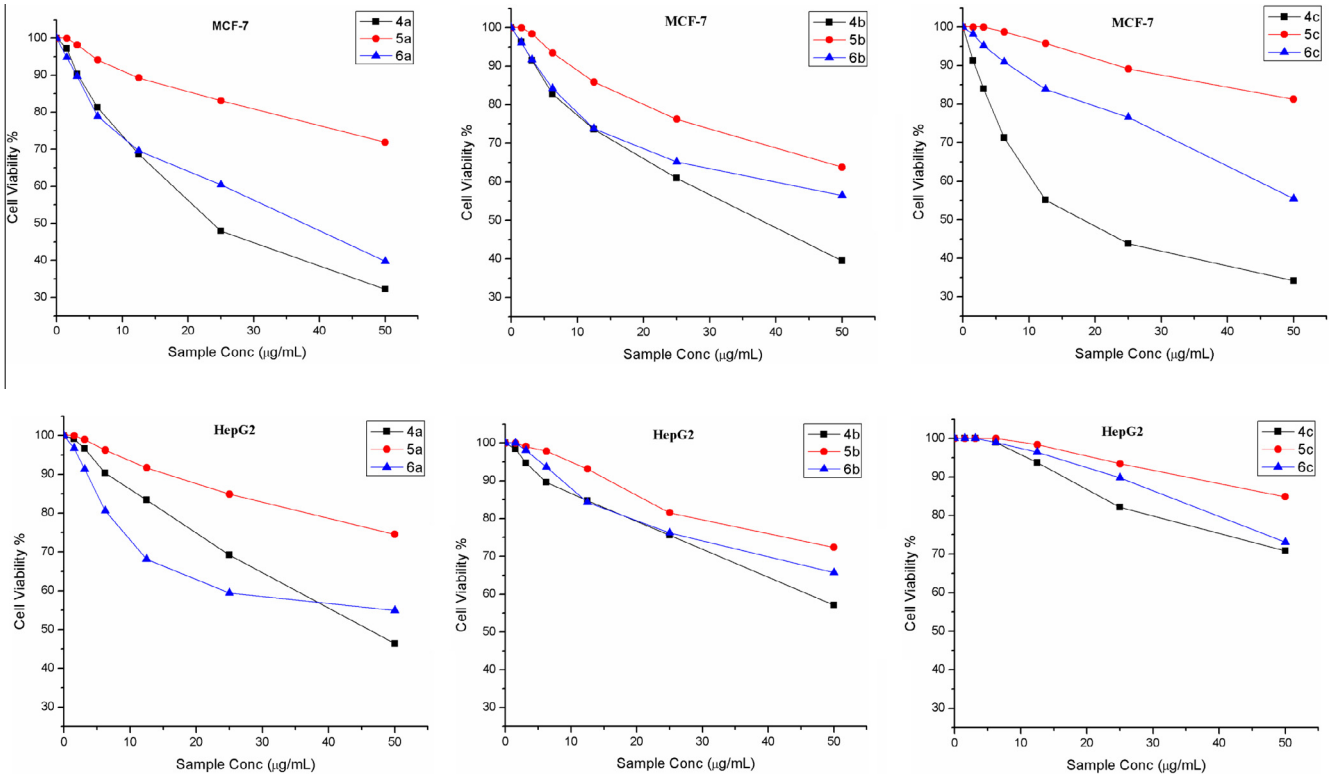

Fig. 3. Concentration dependent analysis of cytotoxic effects of the bis-($Me_2Im^+X^-$)saldach salts (**4**a–c) and their metal complexes (**5**,**6**a–c) on the human MCF-7 and HepG-2 cell lines.

Table 1
IC_{50} values of saldach-bis(imidazolium) salts (**4**a–c) and their M(III)-complexes (**5**,**6**a–c) derivatives towards MCF-7 and HepG-2 cell lines.

Compound	IC_{50} (μM) for the tested compounds	
	MCF-7	HepG-2
4a	33.34 ± 2.41	>50
5a	>50	>50
6a	46.30 ± 3.15	>50
4b	40.41 ± 2.89	>50
5b	48.96 ± 3.54	>50
6b	45.86 ± 3.11	>50
4c	22.17 ± 1.33	>50
5c	>50	>50
6c	>50	>50
Doxorubicin	>50	2.21 ± 1.17

(IC_{50} = 40.41 μM). Lipophilicity and/or vulnerability to hydrolytic cleavage seem to be the key structural features leading to the observed anion-dependent cytotoxicity. Interestingly, the antitumor activity of imidazolium salts may be due to their amphiphilic structure, in which the hydrophilic cationic segments, 1,2-dimethylimidazolium, could have strong electrostatic interactions with the phosphate groups of DNA and hydrogen-bonding association between the anions, BF_4^- and PF_6^-, with the DNA bases [54]. Tetrafluoroborate salt, **4**c, is more cytotoxic than hexafluorophosphate analog, **4**b, because of $[BF4]^-$ anions have higher tendency to establish, on average, more hydrogen bonds with the DNA bases than the $[PF6]^-$ anion.

Notably, Fe(III)-saldach-bis-imidazolium (**6**a–c) complexes appeared to be slightly more cytotoxic than Mn(III) analogs (**5**a–c). The IC_{50} values for the parent ligands and their metal complexes suggest that, chelation of the saldach-bis-imdazolium salts to the Mn(III)/Fe(III) ions significantly decreased their cytotoxicity. This is probably because the hydrogen bonding interactions between two phenolic hydroxyl groups of the free ligands and the functional groups positioned to the edges of DNA bases are no longer possible [55]. Notably, a hydrophobic isopropyl substituents at the ortho-position of the phenolic moieties increase the lipophilicity of the molecule and affect the propensity of a ligand to bind to DNA, contributed to the enhanced cytotoxicity [56].

The lower cytotoxic activities of these metal complexes compared to the parent ligands may be assigned to either difference in their mechanism of action, electronic effects and/or the complex geometry. Where coordination metal ion to the ligand compel the cyclohexane ring to lie perpendicular to the plan of complex [57] and may hinder or even prevent their intercalation with DNA nucleobases (Scheme 5). Consequently, Fe(III) and Mn(III) saldach complexes may induce apoptosis via the mitochondrial pathway [58]. Furthermore, Fe(III) complexes are more cytotoxic than Mn(III) complexes due to the ability of iron chelates to generate reactive oxygen species (ROS) [59] that damage-induced signaling cascades in the tumor cells.

4.3.2. Antibacterial screening

The saldach-bis-imidazolium compounds **4**a–c and standards drugs Gentamycin ($C_{21}H_{43}N_5O_7$, 477.596 g/mol), Tetracycline ($C_{22}H_{24}N_2O_8$, 444.435 g/mol), Amoxicillin ($C_{16}H_{19}N_3O_5S$, 365.400 g/mol) were *in vitro* assessed separately for their capacity to inhibit the growth of the pathogenic bacterial strains by observing the inhibitory zone. From the bactericidal activity data, ZOIs (Fig. 4), Table S6 (see Supplementary data) it has been observed that, the selected compounds showed good to moderate activity against bacteria as compared to known standard drugs. All compounds inhibited the growth of Gram-positive strains slightly more effective than Gram-negative strains. This could be ascribed to their cell walls structural differences, where the outer walls of Gram-negative species are more complex than those of Gram-positive organisms, so all tested compounds diffuse easily through the loose outer wall of Gram-positive bacteria. The antibacterial activ-

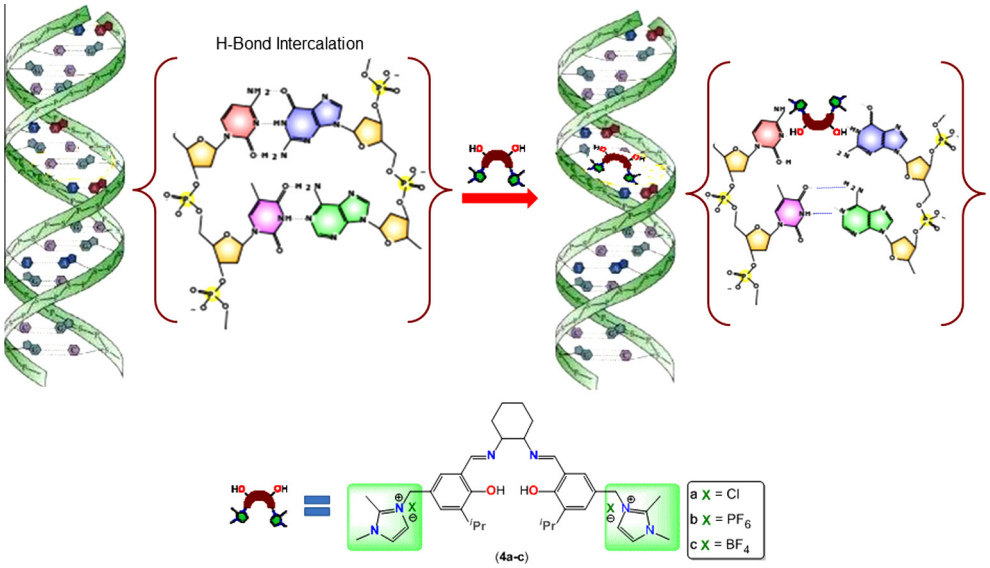

Scheme 5. Hydrogen-bonding of saldach-bis-(imdidazolium) salts to nucleobases in DNA.

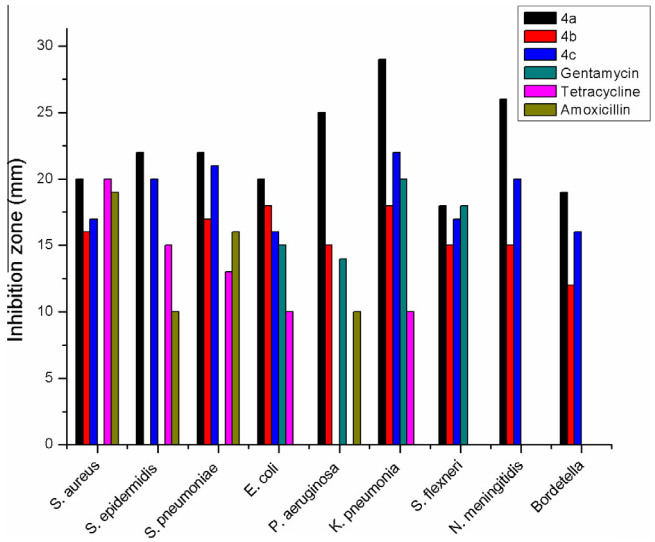

Fig. 4. Graph of zone of inhibition/mm for target compounds against different bacterial species.

ities of the target compounds decrease in the following order: chloride salt of saldach-bis(imidazolium) chloride (**4**a) > hexafluorophosphate (**4**c) > tetrafluoroborate (**4**b). The imidazolium units with chloride anions demonstrate weak antibacterial activity as revealed by higher MIC/MBC values. Exchange of the halide by other anions resulted in an increase of bactericidal and bacteriostatic activities of imidazolium-supported saldach salts. For example, the counterion-dependent antibacterial activity of $H_2(^iPr)_2$saldach(1,2-Me_2Im^+-X^-)$_2$ against *S. aureus* and *E. coli* follows the trend below:

X (MIC/MBC mM)$_{S.\ aureus}$: BF_4 (1.33/4.99) > PF_6 (1.37/ 10.11) > Cl (14.30/ 14.47)

X (MIC/MBC mM)$_{E.\ coli}$: BF_4 (1.35/5.05) > PF_6 (1.39/ 2.58) > Cl (3.50/3.46)

Similar results were obtained by Pernak et al. for imidazolium ionic liquids with an appended alkoxy functional group and anions ([Cl], [BF_4] and [PF_6]) [60].

Also **4**a showed greater antibacterial effect against different bacterial types while **4**b and **4**c exhibited high resistance against *S. pneumoniea* (ATCC 49619) and *P. aeruginosa* (ATCC 27853), respectively.

To investigate growth-inhibitory effects of **4**a–c against *S. aureus* and *E. coli*, the minimum inhibitory concentrations (MIC) and minimum bactericidal concentrations (MBC) were determined by broth dilution method, from the percentages of inhibition at five different concentration levels, 0.12–28.02 mM, and the obtained results are recorded in Table 2. The bacterial growth inhibition is susceptible to the concentration of the compound and the activity is greatly enhanced at the higher concentration. The observed MIC and MBC values for **4**a, **4**b and **4**c against *S. aureus* and *E. coli* revealed that, although **4**a has the greatest antibacterial effect, ZOIs, compared to **4**b and **4**c it needs a high concentration to become bactericidal and can be classified as a new good candidate in the fight against resistant antibiotic bacteria.

The nature of the cell wall, geometry of molecule, positive charge density, hydrophilicity, lipophilicity, pharmacokinetic factors, etc. play decisive roles in determining an antibacterial activity of a Schiff-base and its metal complexes [61]. These factors may lead to enhanced antibacterial activity in two different ways: (i) by interactions of the cationic imidazolium group with the negatively charged microbial cell wall to enhance the bactericidal activity [61], (ii) by the ability of the hydrophobic isopropyl

Table 2
MIC (mM) and MBC (mM) assay results for the saldach-bis-(imdidazolium) salts (**4**a–c) and standard drugs.

Compounds	Bacterium	MIC (mM)	MBC (mM)
4a		14.30±1.88	14.47±2.03
4b	*S. aureus*	1.37 ± 0.31	10.11±0.76
4c	(ATCC 29737)	1.33 ± 0.27	4.99 ± 0.55
Gentamycin		NA	NA
Tetracycline		7.20 ± 0.66	NA
4a		3.50 ± 0.49	3.46 ± 0.47
4b		1.39 ± 0.30	2.58 ± 0.38
4c	*E. coli*	1.35 ± 0.28	5.06 ± 0.61
Gentamycin	(ATCC 10536)	6.70 ± 0.63	NA
Tetracycline		NA	NA

NA = not assigned.

substituents to help to penetrate the lipophilic cell walls and enhance the bactericidal activity [62].

5. Conclusion

In conclusion, a series of water-soluble bis-imidazolium salts, $H_2(^iPr)_2$saldach(1,2-Me_2Im^+-$X^-)_2$, and their Mn(III)/Fe(III) complexes have been prepared. The isolated compounds have been structurally and biologically characterized. NMR and IR spectroscopies affords signatures of the central saldach in the saldach-bis-imidazolium ligands **4**. Ligand **4**a, is in the O-protonated tautomeric form with strong contributions of the ionic, phenolate-iminium tautomer in contrast to the literature on salen and saldach ligands. The aim of this protocol to develop new promising candidates for antibacterial and anticancer chemotherapy. Structure–activity relationships for new compounds against human breast carcinoma (MCF-7) and human hepatocellular carcinoma (HepG2) cell lines revealed a correlation between the hydrophilicity of target compound as tuned by the substituents on the phenolate ligand, and its cytotoxicity and antibacterial activity. The parent ligands (**4**a–c) act as better anticancer and bactericidal agents rather than their complexes ((**5**,**6**)a–c). **4**c (IC_{50} = 19.40 μM) exhibited remarkable results against breast cancer. Also antimicrobial screening showed significant and broad spectrum potency against pathogenic bacterial strains as compared to control drugs. Hence, more distant chemical refinements of the target compounds may serve as a platform towards discovery of exceptionally active antibacterial drug. Notably, exchange of the phenol in the free ligand, by the metal–phenolate bond in the complexes led to an unexpected dramatic decrease in cytotoxic properties. This effect might be a consequence of a reduced degree of the interaction with the specific DNA nucleobase targets though H-bonding.

Acknowledgment

This work was in part supported by DFG grant Ja466/24-1 (initiation of bilateral cooperation RFME-CJ) and DAAD.

Appendix A. Supplementary material

Supplementary data (experimental, spectral and biological data) associated with this article can be found, in the online version, at http://dx.doi.org/10.1016/j.ica.2014.05.029.

References

[1] A. Tanitame, Y. Oyamada, K. Ofuji, M. Fujimoto, K. Suzuki, T. Ueda, H. Terauchi, M. Kawasaki, K. Nagai, M. Wachi, J. Yamagishi, Bioorg. Med. Chem. 12 (2004) 5515.
[2] D.T. Chu, J.J. Plattner, L. Katz, J. Med. Chem. 39 (1996) 3853.
[3] L. Ballell, R.A. Field, K. Duncan, R.J. Young, Antimicrob. Agents Chemother. 49 (2005) 2153.
[4] J.F. Barrett, J.A. Hoch, Antimicrob. Agents Chemother. 42 (1998) 1529.
[5] T. Miyamoto, J. Matsumoto, K. Chiba, H. Egawa, K. Shibamori, A. Minamida, Y. Nishimura, H. Okada, M. Kataoka, M. Fujita, T. Hirose, J. Nakano, J. Med. Chem. 33 (1990) 1645.
[6] N. Nakada, H. Shimada, T. Hirata, Y. Aoki, T. Kamiyama, J. Watanabe, M. Arisawa, Antimicrob. Agents Chemother. 37 (1993) 2656.
[7] (a) K.R. Barnes, S.J. Lippard, Met. Ions Biol. Syst. 42 (2004) 143;
(b) L. Zhang, Y. Zhang, P.Y. Huang, F. Xu, P.J. Peng, Z.Z. Guan, Cancer Chemother. Pharmacol. 61 (2008) 33;
(c) L.J.K. Boerner, J.M. Zaleski, Curr. Opin. Chem. Biol. 9 (2005) 135;
(d) K.I. Ansari, B.P. Mishra, S.S. Mandal, Biochim. Biophys. Acta 1779 (2008) 66;
(e) B. Stordal, N. Pavlakis, R. Davey, Cancer Treat. Rev. 33 (2007) 347.
[8] J.L. Czlapinski, T.L. Sheppard, J. Am. Chem. Soc. 123 (2001) 8618.
[9] I. Ott, R. Gust, Arch. Pharm. (Weinheim) 340 (2007) 117.
[10] (a) G. Sava, S. Zorzet, C. Turrin, E. Vita, M. Soranzo, G. Zabucchi, M. Cocchietto, A. Bergamo, S. DiGiovine, G. Pezzoni, L. Sartor, S. Garbisa, Clin. Cancer Res. 9 (2003) 1898;
(b) P. Köpf-Maier, Eur. J. Clin. Pharmacol. 47 (1994) 1;
(c) P. Köpf-Maier, Anticancer Res. 19 (1999) 493;
(d) C.G. Hartinger, M.A. Jakupec, S. Zorbas-Seifried, M. Groessl, A. Egger, W. Berger, H. Zorbas, P.J. Dyson, B.K. Keppler, Chem. Biodivers. 5 (2008) 2140;
(e) R. Gust, I. Ott, D. Posselt, K. Sommer, J. Med. Chem. 47 (2004) 5837;
(f) B.K. Keppler, M.R. Berger, M.E. Heim, Cancer Treat. Rev. 17 (1990) 261.
[11] (a) S. Bhattacharya, S.S. Mandal, Chem. Commun. (1996) 1515;
(b) C.J. Burrows, R.P. Hickerson, J.G. Muller, B. Felden, S.E. Rokita, Biophys. J. 76 (1999). A5-a5;
(c) J.G. Muller, S.J. Paikoff, S.E. Rokita, C.J. Burrows, J. Inorg. Biochem. 54 (1994) 199;
(d) S. Routier, J.L. Bernier, M.J. Waring, P. Colson, C. Houssier, C. Bailly, J. Org. Chem. 61 (1996) 2326;
(e) D.J. Gravert, J.H. Griffin, J. Org. Chem. 58 (1993) 820;
(f) H.Y. Shrivastava, S.N. Devaraj, B.U. Nair, J. Inorg. Biochem. 98 (2004) 387.
[12] S.E. Rokita, C.J. Burrows, Salen-metal Complexes, Small Molecule DNA and RNA Binders, vol. 1, Wiley-VCH, 2003.
[13] J.G. Muller, L.A. Kayser, S.J. Paikoff, V. Duarte, N. Tang, R.J. Perez, S.E. Rokita, C.J. Burrows, Coord. Chem. Rev. 185–186 (1999) 761.
[14] (a) M. Irisawa, N. Takeda, M. Komiyama, J. Chem. Soc., Chem. Commun. (1995) 1221;
(b) M. Komiyama, N. Takeda, H. Shigekawa, Chem. Commun. (1999) 1443;
(c) D. Prema, A.V. Wiznycia, B.M.T. Scott, J. Hilborn, J. Desper, C.J. Levy, Dalton Trans. 42 (2007) 4496;
(d) A.V. Wiznycia, J. Desper, C.J. Levy, Chem. Commun. 37 (2005) 4693.
[15] G.A. Woldemariam, S.S. Mandal, J. Inorg. Biochem. 102 (2008) 740.
[16] K.I. Ansari, J.D. Grant, G. Woldemariam, S. Kasiri, S.S. Mandal, Org. Biomol. Chem. 7 (2009) 926.
[17] S.R. Doctrow, K. Huffman, C.B. Marcus, G. Tocco, E. Malfroy, C.A. Adinolfi, H. Kruk, K. Baker, N. Lazarowych, J. Mascarenhas, B. Malfroy, J. Med. Chem. 45 (2002) 4549.
[18] Y. Rong, S.R. Doctrow, G. Tocco, M. Baudry, Proc. Natl. Acad. Sci. U.S.A. 96 (1999) 9897.
[19] K.I. Ansari, J.D. Grant, S. Kasiri, G. Woldemariam, B. Shrestha, S.S. Mandal, J. Inorg. Biochem. 103 (2009) 818.
[20] W.L. Hough, M. Smiglak, H. Rodrıguez, R.P. Swatloski, S.K. Spear, D.T. Daly, J. Pernak, J.E. Grisel, R.D. Carliss, M.D. Soutullo, New J. Chem. 31 (2007) 1429.
[21] K.M. Hindi, M.J. Panzner, C.A. Tessier, C.L. Cannon, W.J. Youngs, Chem. Rev. 109 (2009) 3859.
[22] (a) J. Pernak, I. Goc, I. Mirska, Green Chem. 6 (2004) 323;
(b) D. Demberelnyamba, K.-S. Kim, S. Choi, S.Y. Park, H. Lee, C.J. Kim, I.D. Yoo, Bioorg. Med. Chem. 12 (2004) 853;
(c) J. Pernak, K. Sobaszkiewicz, I. Mirska, Green Chem. 5 (2003) 52;
(d) J. Pernak, K. Sobaszkiewicz, J. Foksowicz-Flaczyk, Chem. Eur. J. 10 (2004) 3479.
[23] F. Stock, J. Hoffman, J. Ranke, B. Ondruschka, B. Jastorff, Green Chem. 6 (2004) 286.
[24] A.C. Skladanowski, P. Stepnowski, K. Kleszczynski, B. Dmochowska, Environ. Toxicol. Pharmacol. 19 (2005) 291.
[25] F. Hosseinzadeh, M. Mahkam, M. Galehassadi, Des. Monomers Polym. 15 (2012) 379.
[26] S. Budagumpi, R.A. Haque, S. Endud, G. Ur, Eur. J. Inorg. Chem. (2013) 4367;
(a) A. Gautier, F. Cisnetti, Metallomics 4 (2012) 23;
(b) S.V. Malhotra, V. Kumar, Bioorg. Med. Chem. Lett. 20 (2010) 581.
[27] (a) K. Fujita, D.R. MacFarlane, M. Forsyth, Chem. Commun. (2005) 4804;
(b) J. Von Hagen, U. Michelsen, U.S. Patent US7470778B2, 2008.
[28] L. Carson, P.K.W. Chau, M.J. Earle, M.A. Gilea, B.F. Gilmore, S.P. Gorman, M.T. McCann, K.R. Seddon, Green Chem. 11 (2009) 492.
[29] (a) K.M. Docherty, C.F. Kulpa, Green Chem. 7 (2005) 185;
(b) M.T. Garcia, N. Gathergood, P.J. Scammells, Green Chem. 7 (2005) 9;
(c) P.J. Scammels, J.L. Scott, R.D. Singer, Aust. J. Chem. 58 (2005) 155;
(d) N. Gathergood, P.J. Scammels, Aust. J. Chem. 55 (2002) 557;
(e) J. Łuczak, C. Jungnickel, I. Łacka, S. Stolte, J. Hupka, Green Chem. 12 (2010) 593.
[30] (a) S. Budagumpi, R.A. Haque, A.W. Salman, M.Z. Ghdhayeb, Inorg. Chim. Acta 392 (2012) 61;
(b) A.W. Salman, R.A. Haque, S. Budagumpi, H.Z. Zulikha, Polyhedron 49 (2013) 200.
[31] (a) R.F.M Elshaarawy, Synthesis and reactions of some pyridoyl derivatives with anticipated biological activities (M.Sc. thesis) Suez Canal university, Egypt, 2001.;
(b) B. Wisser, C. Janiak, Z. Anorg. Allg. Chem. 633 (2007) 1796;
(c) R.F.M. Elshaarawy, H.K. Ibrahim, E. Eltamany, I. Mohy-Eldeen, Maced. J. Chem. Chem. Eng. 27 (1) (2008) 65;
(d) A.-C. Chamayou, M.A. Neelakantan, S. Thalamuthu, C. Janiak, Inorg. Chim. Acta 365 (2011) 447.
[32] (a) T. Mosmann, J. Immunol. Methods 65 (1983) 55;
(b) P. Vijayan, C. Raghu, G. Ashok, S.A. Dhanaraj, Indian J. Med. Res. 120 (2004) 24.
[33] C. Perez, P.M. Bazerque, Acta Biol. Med. Exp. 15 (1990) 113.
[34] A.J. Vlietink, L. Van Hoof, J. Totte, H. Laure, D.V. Berhe, P.C. Rwangabo, J. Mrukiyunmwami, J. Ethnopharm. 46 (1995) 31.
[35] R.F.M. Elshaarawy, C. Janiak, Eur. J. Med. Chem. (in press).
[36] A. Hille, I. Ott, A. Kitanovic, I. Kitanovic, H. Alborzinia, E. Lederer, S. Wölfl, N. Metzler-Nolte, S. Schäfer, W.S. Sheldrick, C. Bischof, U. Schatzschneider, R. Gust, J. Biol. Inorg. Chem. 14 (2009) 711.
[37] M.J. Sabater, A. Corma, J.V. Folgado, H. Garcia, J. Phys. Org. Chem. 13 (2000) 57.

[38] C. Núñez, R. Bastida, A. Macías, L. Valencia, J. Ribas, J.L. Capelo, C. Lodeiro, Dalton Trans. 39 (2010) 7673.
[39] M.M. Stone, A.H. Franz, C.B. Lebrilla, J. Am. Soc. Mass Spectrom. 13 (2002) 964.
[40] M. Azam, Z. Hussain, I. Warad, S.I. Al-Resayes, M.S. Khan, M. Shakir, A. Trzesowska-Kruszynskae, Dalton Trans. 41 (2012) 10854.
[41] M.R. Mauryaa, A.K. Chandrakar, S. Chand, J. Mol. Catal. A 270 (2007) 225.
[42] (a) Webster F.X., Silverstein R.M., Spectrophotometer Identification of Organic Compounds, vol. 87, sixth ed., John Wiley, New York, 1992.;
(b) O. Pouralimardan, A.-C. Chamayou, C. Janiak, H.H. Monfared, Inorg. Chim. Acta 360 (2007) 1599;
(c) R.I. Kureshy, K.J. Prathap, T. Roy, N.C. Maity, N.H. Khan, S.H.R. Abdi, H.C. Bajaj, Adv. Synth. Catal. 352 (2010) 3053;
(d) T. Chang, L. Jin, H. Jing, ChemCatChem 1 (2009) 379.
[43] (a) K. Nakomoto, Infrared and Raman Spectroscopy of Inorganic and Coordination Compounds, third ed., Wiley Interscience, New York, 1978;
(b) R.F.M. Elshaarawy, Y. Lan, Inorg. Chim. Acta 401 (2013) 85;
(c) G. Karimipour, M. Montazerozohori, N.H. Naeini, Iran. J. Chem. Chem. Eng. 30 (2011) 13;
(d) X. Guojin, W. Saili, F. Yingguo, Z. Libo, T. Yuhai, Z. Yuansuo, Chin. J. Catal. 33 (2012) 473.
[44] (a) K. Kurzak, I. Kuzniarska-Biernacka, B. Zurowska, J. Solution Chem. 28 (1999) 133;
(b) O.T. Benjelloun, M. Akkurt, S.Ö. Yıldırım, M. Daoudi, N. BenLarbi, A. Kerbal, B. Ben nani, O. Büyükgüngör, A.F. Jalbout, T. Ben Hadda, ARKIVOC xi (2008) 56;
(c) B.M. Drašković, G.A. Bogdanović, M.A. Neelakantan, A.-C. Chamayou, S. Thalamuthu, Y.S. Avadhut, J. Schmed tauf der Günne, S. Banerjee, C. Janiak, Cryst. Growth Des. 10 (2010) 1665;
(d) A. Blagu, D. Cinčić, T. Friščić, B. Kaitner, V. Stilinović, Maced. J. Chem. Chem. Eng. 29 (2010) 117.
[45] (a) Ĕ. Tozzo, S. Romera, M.P. dos Santos, M. Muraro, J. Mol. Struct. 876 (2008) 110;
(b) P.J.K. Inba, B. Annaraj, S. Thalamuthu, M.A. Neelakantan, Spectrochim. Acta A 104 (2013) 300.
[46] (a) N.B. Pahor, M. Calligaris, P. Delise, G. Dodic, G. Nardin, L. Randaccio, Dalton Trans. (1976) 2478;
(b) K. Lippe, D. Gerlach, E. Kroke, Organometallics 28 (2008) 621;
(c) A. Dalla Cort, F. Gasparrini, L. Lunazzi, L. Mandolini, A. Mazzanti, C. Pasquini, M. Pierini, R. Rompietti, L. Schiaffino, J. Org. Chem. 70 (2005) 8877;
(d) C.-G.F. von Richthofen, A. Stammler, H. Bögge, T. Glaser, J. Org. Chem. 77 (2012) 1435.
[47] R.M. Claramunt, J Prog. Nucl. Magn. Reson. Spectrosc. 49 (2006) 169.
[48] S.H. Alarcon, A.C. Olivieri, M. Gonzalez-Sierra, J. Chem. Soc., Perkin Trans. (1994) 1067.
[49] D.M. Boghaei, S. Mohebi, J. Chem. Res. Synop. (2002) 72.
[50] (a) S.M. Crawford, Spectrochim. Acta 19 (1963) 255;
(b) B. Bosnich, J. Am. Chem. Soc. 90 (1968) 627;
(c) S. Di Bella, I. Fragala, I. Ledoux, M.A. Diaz-Garcia, T.J. Marks, J. Am. Chem. Soc. 119 (1997) 9550.
[51] L.J. Boucher, M.O. Farrell, J. Inorg. Nucl. Chem. 35 (1973) 3731.
[52] B.P. Gaber, V. Miskowski, T.G. Spiro, J. Am. Chem. Soc. 96 (1974) 6868.
[53] O. Kahn, Molecular Magnetism, VCH, New York, 1993.
[54] L. Cardoso, N.M. Micaelo, ChemPhysChem 12 (2011) 275.
[55] S. Tabassum, M. Zaki, M. Afzal, F. Arjmand, Dalton Trans. 42 (2013) 10029.
[56] N. Berthet, V. Martel-Frachet, F. Michel, C. Philouze, S. Hamman, X. Ronotb, F. Thomas, Dalton Trans. 42 (2013) 8468.
[57] A. Hille, R. Gust, Arch. Pharm. Chem. Life Sci. 342 (2009) 625.
[58] (a) K.I. Ansari, J.D. Grant, G.A. Woldemariam, S. Kasiri, S.S. Mandal, Org. Biomol. Chem. 7 (2009) 926;
(b) K.I. Ansari, S. Kasiri, J.D. Grant, S.S. Mandal, Dalton Trans. (2009) 8525;
(c) K.I. Ansari, J.D. Grant, S. Kasiri, G.A. Woldemariam, B. Shrestha, S.S. Mandal, J. Inorg. Biochem. 103 (2009) 818.
[59] A. Hille, I. Ott, A. Kitanovic, I. Kitanovic, H. Alborzinia, E. Lederer, J. Biol. Inorg. Chem. 14 (2009) 711.
[60] J. Pernak, K. Sobaszkiewicz, I. Mirska, Green Chem. 5 (2003) 52.
[61] (a) M. Kong, X.G. Chen, K. Xing, H.J. Park, Int. J. Food Microbiol. (2010) 51;
(b) V.P. Daniel, B. Murukan, B.S. Kumari, K. Mohanan, Spectrochim. Acta A 70 (2008) 403.
[62] E.I. Rabea, M.E.I. Badawy, T.M. Rogge, C.V. Stevens, M. Höfte, W. Steurbaut, G. Smagghe, Pest Manag. Sci. 61 (2005) 951.